Conceptual Plan:
Two-Phase Flow Laboratory Program
for the Waste Isolation Pilot Plant

Susan M. Howarth
Fluid Flow and Transport Department 6115
Sandia National Laboratories
Albuquerque, NM 87185

ABSTRACT

The Salado Two-Phase Flow Laboratory Program was established to address concerns regarding two-phase flow properties and to provide WIPP-specific, geologically consistent experimental data to develop more appropriate correlations for Salado rock to replace those currently used in Performance Assessment models. Researchers in Sandia's Fluid Flow and Transport Department originally identified and emphasized the need for laboratory measurements of Salado threshold pressure and relative permeability. The program expanded to include the measurement of capillary pressure, rock compressibility, porosity, and intrinsic permeability and the assessment of core damage. Sensitivity analyses identified the anhydrite interbed layers as the most likely path for the dissipation of waste-generated gas from waste-storage rooms because of their relatively high permeability. Due to this the program will initially focus on the anhydrite interbed material. The program may expand to include similar rock and flow measurements on other WIPP materials including impure halite, pure halite, and backfill and seal materials.

This conceptual plan presents the scope, objectives, and historical documentation of the development of the Salado Two-Phase Flow Program through January 1993. Potential laboratory techniques for assessing core damage and measuring porosity, rock compressibility, capillary and threshold pressure, permeability as a function of stress, and relative permeability are discussed. Details of actual test designs, test procedures, and data analysis are not included in this report, but will be included in the Salado Two-Phase Flow Laboratory Program Test Plan pending the results of experimental and other scoping activities in FY93.

MASTER

ACKNOWLEDGMENTS

CONTENTS

CONTENTS (Continued)

Figures

Tables

1.0 SUMMARY

The Salado Two-Phase Flow Laboratory Program was established in January 1992 to measure threshold pressure and relative permeability for Salado rock in the laboratory. FY92 scoping activities focussed on investigating Waste Isolation Pilot Plant (WIPP) program needs in the area of two-phase flow and assessing current laboratory measurement technology. As a result of the FY92 scoping activities, the Salado Two-Phase Flow Laboratory Program was expanded to include measurement of capillary pressure, single-phase permeability as a function of stress, total and effective porosity, rock compressibility, and the investigation of coring-induced damage in addition to threshold pressure and relative permeability. FY93 experimental scoping activities are designed to characterize the Salado anhydrite rock and measure single-phase flow properties in the laboratory. Information gained from these initial tests will be used to design and implement two-phase flow measurement tests including threshold pressure, capillary pressure, and relative permeability scheduled to begin in FY94. These measurements support the development of the numerical models used to predict the long-term hydrologic and structural response of the WIPP repository to waste-generated gas, an activity critical for assessing the long-term performance of the repository.

This report presents the scope, objectives, and milestone schedule for the Salado Two-Phase Flow Laboratory Program. In addition, this report documents the development of the Salado Two-Phase Flow Program through January 1993. Current laboratory techniques for assessing core damage and measuring porosity, capillary and threshold pressure, permeability, rock compressibility, and relative permeability are also discussed. Research and experimental scoping activities will continue throughout FY93 to determine the specific experiments to be performed. Details of actual test designs and procedures for each experiment and data analysis are not included in this report, but will be included in the Two-Phase Flow Laboratory Program Test Plan.

2.0 INTRODUCTION

2.1 Background

The WIPP is the U.S. Department of Energy's (DOE's) planned repository for transuranic waste generated by our nation's defense programs. This underground research and development effort is generating the technology base for the safe disposal of radioactive wastes in bedded salt. The Salado Formation was chosen for the repository because of salt's natural ability to creep under the effects of stress and ultimately to encapsulate and isolate the waste. A significant part of this effort is to develop a numerical capability to predict the hydrologic and structural response of a bedded salt repository, an activity critical for assessing the long-term performance of the facility.

The Salado Formation consists of thick halite layers with interbeds of minerals such as clay and anhydrite. The polycrystalline Salado salt contains small quantities of brine in intragranular fluid inclusions and as intergranular (pore) fluid. The anhydrite interbed layers also contain small quantities of brine. It is important to quantify the amount of brine in the Salado Formation and determine its mobility and flow properties because the accumulation of significant quantities of brine in the repository could potentially lead to problems that affect the salt's ability to isolate waste. One such problem is gas generation from the microbial degradation of organic waste and anoxic corrosion of steel drums and metallic waste in the presence of brine. Waste-generated gas may be produced in quantities sufficient to reach high pressures and retard the natural flow or creep effects of the salt. Potential negative impacts of high room pressure are that (1) waste-generated gas may serve as an additional driving force and push contaminated brine far out into the formation, and (2) the high pressure may fracture the formation and result in increased permeability of the transport pathways.

From a technical point of view, we need to quantify the Salado rock and flow parameters that describe its ability to transmit and store fluids as a function of the initial conditions and

time-dependent material damage. For example, permeability data from in situ tests indicate that the anhydrite and impure halite interbeds within the Salado Formation have higher permeability, by 1 to 2 orders of magnitude, than the pure halite intervals. Sensitivity analyses show that the anhydrite interbeds could be the primary inward flow path for brine to the repository and outward flow path for waste-generated gas into the formation (Davies et al., 1991). Thus, the role of the anhydrite marker beds in the long-term hydrological response of the WIPP facility has become an issue that revolves around (1) the initial state of the material, (2) the mechanism(s) and potential for brine and gas flow in the material, and (3) the influence of excavation-induced damage on these flow parameters (if only to be able to separate damaged from undamaged behavior). There are a number of laterally continuous anhydrite interbeds within the Salado Formation in the vicinity of the repository horizon including Marker Beds 138 and 139 and anhydrites "a" and "b."

One anhydrite interbed that forms a potential gas flow path is the 1-meter (m) thick Marker Bed (MB) 139, which lies approximately 1 m below the planned waste storage rooms. MB 139 is one of about 45 siliceous or sulfatic units within the Salado Formation consisting of polyhalitic anhydrite. Permeability values of 5×10^{-17} to 8×10^{-20} m^2 have been inferred from eight in situ borehole tests in MB 139 (Davies et al., 1992). To date, laboratory examination and testing of the anhydrite interbed material is extremely limited.

The flow of waste-generated gas from the repository is predicted to be controlled by three physical properties of the surrounding rock (Davies, 1991): (1) pore fluid pressure, (2) threshold displacement pressure, and (3) gas-brine relative permeability. Flow of waste-generated gas into the Salado Formation surrounding the repository will occur only when the gas pressure (P_{gas}) in the repository exceeds the sum of the formation near-field pore fluid pressure (P_p) and the formation's threshold pressure (P_t) as described in Equation 1. This pressure, P_{gas}, is termed the gas-threshold displacement pressure.

$$P_{gas} > P_p + P_t \quad .$$

(1)

4

Pore fluid pressure (P_p), also referred to herein as pore pressure, is defined as the pressure of the fluid (brine) within the rock's pore space. The pore fluid pressure in the undisturbed regions of the Salado Formation is expected to range between hydrostatic and lithostatic, 6.4 MPa (pure water, 1 gm/cm³) to 14.8 MPa (rock, 2.32 gm/cm³), because the pore fluid may partially support the load of the 655 m of rock overlying the repository (Figure 1). Pore pressure inferred from in situ permeability test data in the Salado far-field and undisturbed regions ranges from 9.5 to 12.6 MPa (see Appendix A). As expected and exhibited in Group 2 shown in Table 1, pore pressures measured in the depressurized and disturbed regions are significantly lower because of flow into the repository, excavation-induced stress changes, and possible dilatation effects (Davies, 1991; Davies et al., 1992).
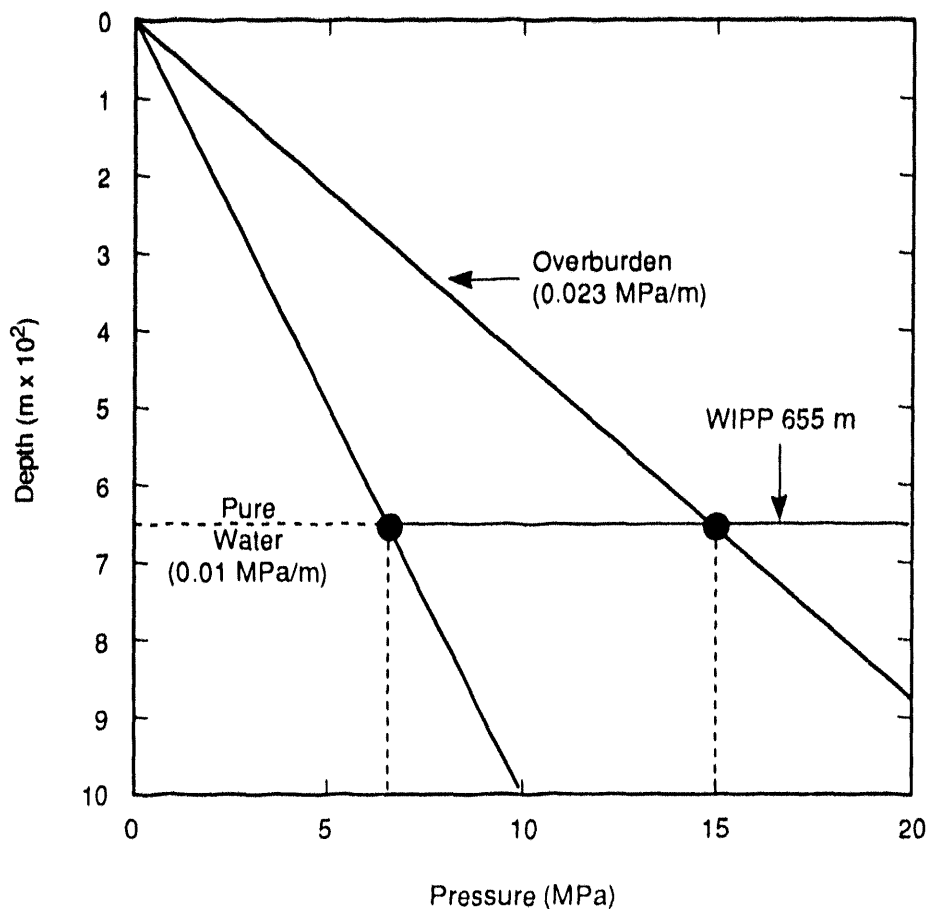
TRI-6119-122-0

Figure 1. Pore fluid pressure versus depth.

5

Table 1. Experimental Data from Permeability Testing of Anhydrite Interbeds
(Davies et al., 1992)

Group 1: No substantial formation fluid depressurization			
Test	Unit	Permeability (m²)	PorePressure(MPa)
SCP01	MB139	3.0×10^{21}	12.4
QPP13	Pre-mineby MB139	4.1×10^{21}	12.5
QPP03	Pre-mineby anhydrite "b"	4.4×10^{21}	12.6

Group 2: Moderate formation fluid depressurization			
Test	Unit	Permeability (m²)	PorePressure(MPa)
C2H02	MB139	7.8×10^{21}	9.3
L4P51-B	Anhydrite "c"	5.0×10^{21}	5.1
S1P71-B	Anhydrite "c"	6.8×10^{21}	4.9
C2H01-C	MB139	9.5×10^{21}	8.0
C1X10	MB139	5.0×10^{21}	7.3
QPP03	Anhydrite "b" post-mineby	7.9×10^{21}	7.0
QPP13	MB139 post-mineby	4.7×10^{21}	8.1
L4P52-A	Anhydrite "a"	1.0×10^{21}	6.4
QPB01	MB139	9.6×10^{21}	5.0 assumed
QPB02	MB139	1.6×10^{21}	5.0 assumed
QPB03	MB139	1.2×10^{21}	5.0 assumed

Gas threshold displacement pressure ($P_{g,n}$) is defined as the minimum pressure at which a nonwetting phase fluid (waste-generated gas) can overcome pore pressure and capillary effects, enter a 100 percent wetting-phase-fluid saturated porous medium, and cause displacement of the wetting-phase fluid (brine in the Salado Formation). Capillary effects are quantified as capillary pressure (P_c), which for high-permeability rocks, is typically measured directly on core samples in the laboratory.

Threshold pressure (P_t) is related to the capillary-pressure characteristic curve as shown in Figure 2 and is defined as either (1) the endpoint pressure on the capillary pressure-versus-wetting-phase saturation curve corresponding to a wetting-phase saturation of 1.0, or (2) the pressure on the capillary pressure-versus-wetting-phase saturation curve corresponding to the nonwetting phase critical saturation. The first definition applies to *initial penetration* of the nonwetting phase fluid into the wetting-phase saturated porous medium; the second applies to the development of a nonwetting phase continuum through the core and *initial breakthrough* of nonwetting-phase fluid (Davies, 1991).
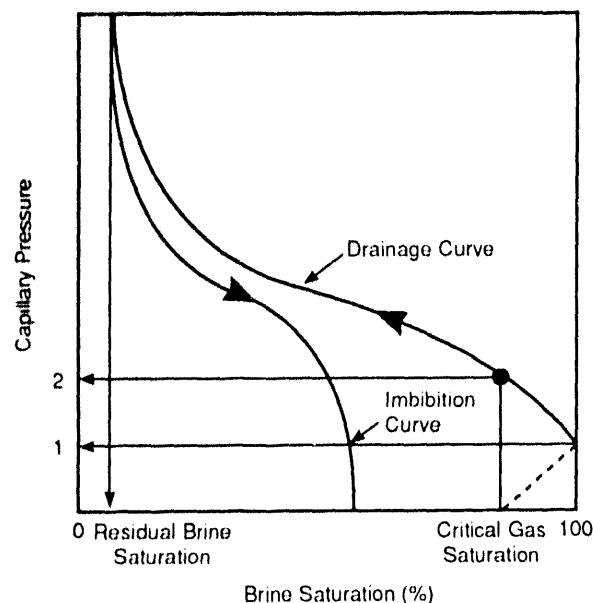
Figure 2. Capillary pressure versus saturation.

7

Whereas absolute or intrinsic permeability (k) is a measure of the rate at which a single fluid will flow through interconnected pores (single- or one-phase flow), relative permeability relationships must be considered when evaluating flow properties of more than one fluid in porous media. Relative permeability (k_r) compares the rate at which a fluid will move through interconnected pore space when another fluid is present: gas flowing in the presence of brine. Relative permeability is especially important in WIPP performance-assessment calculations because prediction of repository behavior, such as brine inflow to repository rooms and gas outflow to the formation, is strongly dependent upon this parameter.

2.2 Rationale

Pore pressure is measured in situ as part of the Large-Scale Brine Inflow Experiment (Room Q) and the Permeability Testing Program, and preparations are being made for the first in situ threshold pressure test. However, neither threshold pressure nor relative permeability has been measured on Salado cores in the laboratory, so the Brooks and Corey (1964) and Parker et al. (1987) correlations are used in the current WIPP Performance Assessment (PA) models for these parameters. These two models are based upon capillary pressure relationships from which wetting-phase relative permeability is derived (Webb, 1992).

The Brooks and Corey (1964) relationship for capillary pressure (Equation 2) is expressed below in terms of effective saturation, S_e; threshold pressure, P_t at $S_c = 1.0$; and pore-size distribution parameter, λ. Effective saturation is a function of the wetting- and nonwetting-phase fluid saturations, S_w and S_{nw}, and the wetting- and nonwetting-phase fluid residual saturations, $S_{w,r}$ and $S_{nw,r}$.

$$P_c = \frac{P_t}{S_e^{1/\lambda}} \tag{2}$$

8

where

$$S_e = \frac{S_w - S_{w,r}}{1 - S_{nw,r} - S_{w,r}} \quad . \tag{3}$$

The Brooks and Corey (1964) correlation is intended for use only over that portion of the capillary pressure curve where P_c is greater than the pressure corresponding to $S_e = 1.0$.

Similarly, the Parker et al. (1987) relationship for capillary pressure (Equation 4) is expressed in terms of a reference pressure, P_o; effective saturation, S^*; and a pore-size distribution parameter, m. The Parker et al. (1987) equation differs from the Brooks and Corey (1964) equation in that the former assumes that threshold pressure is zero and effective saturation is a function of the minimum wetting-phase saturation, $S_{w,m}$. All other terms are the same as those defined for the Brooks and Corey (1964) relationship.

$$P_c = P_o (S^{*^{-1/m}} - 1)^{1-m} \tag{4}$$

where

$$S^* = \frac{S_w - S_{w,r}}{S_{w,m} - S_{w,r}} \quad . \tag{5}$$

Both the Brooks and Corey (1964) and Parker et al. (1987) correlations used in current WIPP PA numerical models were developed using data from one core sample analyzed for the Tight Gas Sands project. The pore-size distribution parameter, λ, and residual non-wetting phase saturation are based upon data from a single core, MWX-3 67-35, described in Rechard et al. (1990) and Morrow et al. (1986). Other input values to these models include threshold pressure, residual wetting-phase saturation, and minimum wetting-phase saturation.

9

None of the input values to the Brooks and Corey (1964) and Parker et al. (1987) correlations has been measured for the Salado Formation rock. The validity of using correlations based on tight gas sands data to predict Salado threshold pressure, capillary pressure, and relative permeability has not been experimentally justified; the tight gas sands data are simply the closest analog for which detailed data are available. In addition, detailed laboratory measurements of anhydrite capillary pressure and relative permeability made over a wide range of saturations would support interpretation of the in situ permeability tests.

Uncertainty in expected threshold displacement pressure values for the Salado Formation is large, and estimates range from 0.5 to 50 MPa depending upon lithology (Davies, 1991). This wide range of values may prevent a clear prediction of repository behavior in both the undisturbed and human-intrusion WIPP PA scenarios. Credibility of the two-phase hydrologic modeling in support of PA relies on measurement of this sensitive Salado Formation parameter. Threshold displacement-pressure measurements in the laboratory and/or field will provide data to support the development and evaluation of Salado models and performance-assessment calculations.

In summary, the work of both Davies and Webb emphasized the need for investigating and measuring capillary and threshold pressure and relative permeability of Salado rock. Subsequent scoping activities showed that other related parameters including porosity, rock compressibility, and intrinsic permeability should also be measured to support WIPP Performance Assessment and Fluid Flow and Transport numerical modelers and analysts. The anhydrite interbed layers were identified as the most likely path for the dissipation of waste-generated gas from waste storage rooms because of their relatively high permeability and likely low threshold displacement pressure. In addition to the interbed layers, two-phase measurements may be needed for impure halite, pure halite, backfill material, and possibly seal material.

2.3 Related Work

The primary objective of this test program is to measure two-phase flow properties for the anhydrite interbeds at WIPP. To make these measurements properly, fundamental rock properties, including porosity, rock compressibility, and intrinsic (single-phase) permeability, should first be measured and the issue of coring-induced damage should be addressed. Work associated with the WIPP in areas pertinent to those described in this conceptual plan include sensitivity studies, laboratory studies, and field studies.

2.3.1 Sensitivity Studies

The combined effect of waste-generated gas and high gas-threshold displacement pressure in the Salado was identified as a WIPP PA issue by John Bredehoeft and George Hornberger at the June 1989 National Academy of Sciences (NAS) WIPP Panel Meeting (Davies, 1991). In response to concerns that waste-generated gas pressure might exceed lithostatic pressure and cause unpredictable fracturing, Davies (1989) provided threshold pressure estimates and preliminary two-phase waste-gas and brine-flow simulations. In their September 1990 presentation to the NAS, Davies et al. (1990) identified two-phase properties of Salado interbeds and sensitivity to these properties as important sources of uncertainty that may affect room pressurization.

Davies (1991) followed with a report evaluating the role of threshold pressure in controlling the flow of waste-generated gas into the Salado Formation. In that report, he provided estimates of Salado threshold pressure as a function of lithology, and as shown in Figure 3a and b, he found that threshold pressure increases with decreasing permeability. Davies identified the nonhalite interbeds as the likely dominant flow paths for waste-generated gas from a pressurized repository because of their relatively high permeability and correspondingly low gas threshold pressure. In providing estimates for Salado threshold pressure, he cautioned that the values were based upon information for nonsalt rock types and

that they "must be confirmed with in situ or laboratory measurements that are specific to the Salado Formation at the WIPP repository" (Davies, 1991).

Webb (Davies et al., 1991) performed sensitivity analyses to determine the effect of formation permeability, two-phase (relative permeability and capillary pressure) characteristic curves, and other variations on the long-term performance of the repository. In particular, he focussed upon identifying the dominant variables influencing pressurization of the repository and gas migration distance. Webb found that relative permeability and the residual saturation can have a dramatic effect on the gas migration distance. Likewise, he found that formation permeability can have a dramatic effect upon peak room pressure.
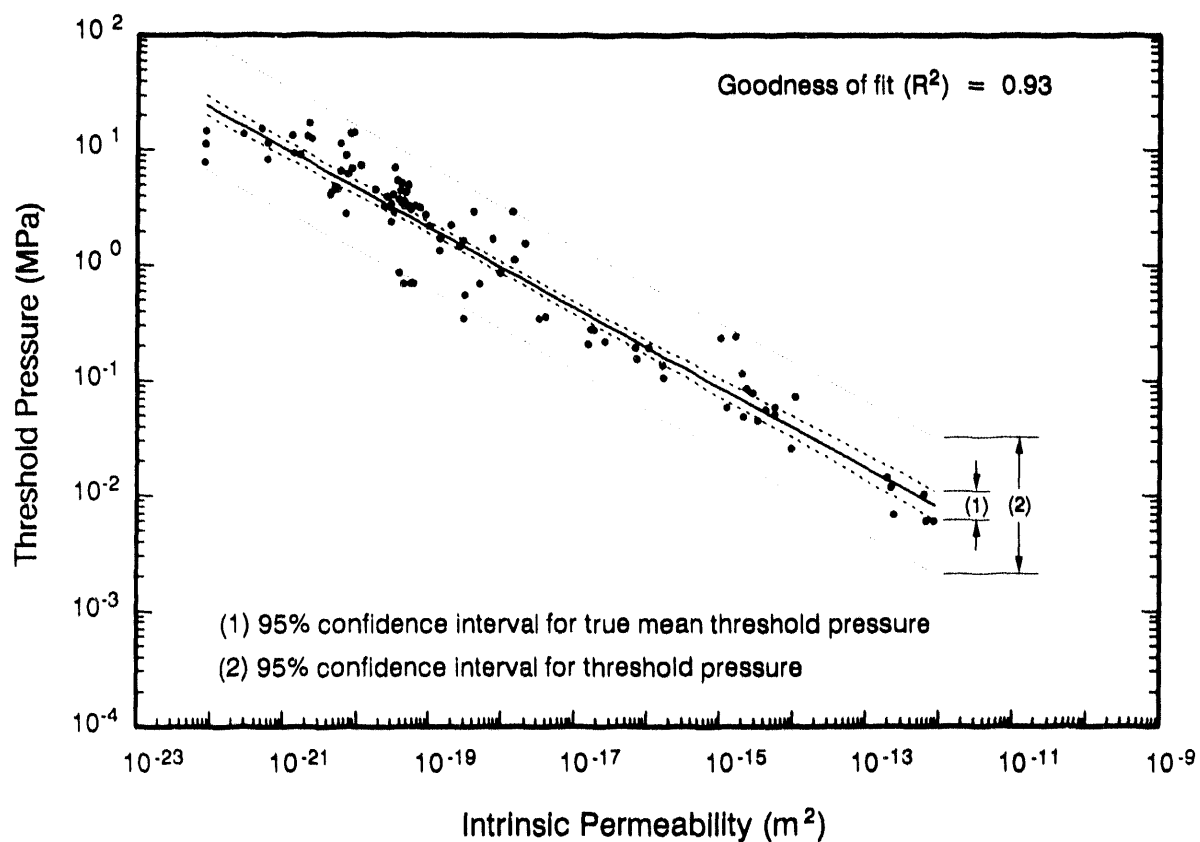
TRI-6344-730-0

Figure 3a.   Plot of correlation of threshold pressure with intrinsic permeability for a composite of data from all consolidated rock lithologies (Davies, 1991).

Intrinsic Permeability (m²)	Estimated Threshold Pressure (MPa)	Salado Formation Lithology (Far-Field)	Disturbed Rock Zone (Near-Field)
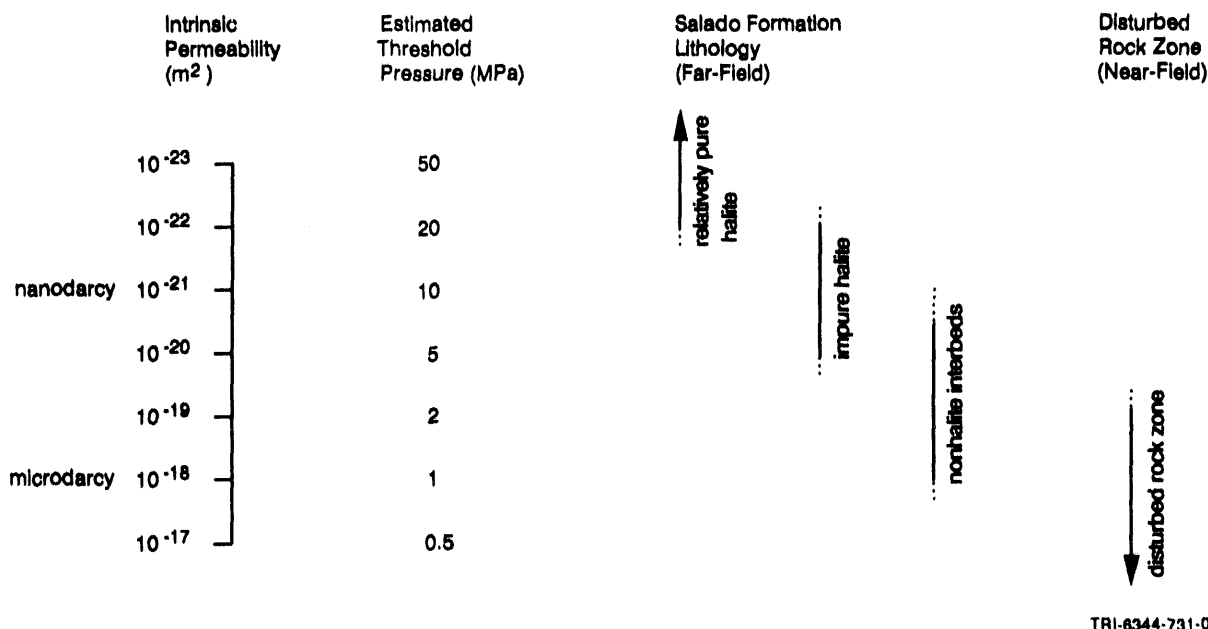
Figure 3b.   Plot summarizing estimated threshold pressure for various lithologic units in the Salado Formation based on correlation with intrinsic permeability (Davies, 1991).

2.3.2 Laboratory Studies

Characterization of core damage, fractures, porosity, permeability, relative permeability, and capillary and threshold pressure are performed routinely in the laboratory. The techniques used to make these laboratory assessments were developed to support the petroleum industry in providing data to quantify oil and gas reserves and optimize reservoir productivity. In 1960, the American Petroleum Institute (API) set standards and guidelines for measuring porosity and intrinsic permeability on rock core samples. While these original standards for measuring rock and single-phase flow properties are being updated as a result of technological advances, the revised guidelines are not expected to include any references to relative permeability, threshold pressure, or capillary pressure measurements. The Society of Core Analysts (SCA) recognized this oversight and initiated a program in 1992 to establish guidelines for laboratory measurement of threshold and capillary pressure and relative permeability. The SCA study is still in progress, and guidelines have not been published.

13

Because no formal standards or guidelines exist for measuring threshold and capillary pressure or relative permeability, especially in low-permeability media, it is necessary to evaluate current laboratory techniques for these measurements to determine the most appropriate one(s) to use within the scope of the Two-Phase Flow Laboratory Program. Investigation and determination of appropriate methods for making these measurements will be addressed in two separate reports: (1) Evaluation of Experimental Techniques to Measure Threshold Pressure for the Salado Formation Anhydrite Interbeds at the Waste Isolation Pilot Plant, and (2) Evaluation of Experimental Techniques to Measure Relative Permeability for the Salado Formation Anhydrite Interbeds at the Waste Isolation Pilot Plant. Laboratory techniques under consideration for assessing core damage and measuring single- and two-phase rock and flow properties within the scope of the Salado Two-Phase Flow Program are discussed in Section 5.0.

2.3.2.1 LABORATORY PERMEABILITY TESTS ON ANHYDRITE INTERBED MATERIAL

The only permeability tests performed on Salado anhydrite interbed material to date were done as part of the Site Validation Experiments in 1983 (Black et al., 1983). Gas permeability (single-phase) measurements were made on three anhydrite core samples in the laboratory at the Waterways Experiment Station, U.S. Army Corps of Engineers, Vicksburg, MS. All three cores (HPC 1, HPC 2, and HPC 3) were taken from a single hole, approximately 64-cm deep, located in the outer rib of the E140 drift at the WIPP. The report describes the material only as "interbed" and reveals nothing in terms of specific stratigraphic unit or mineralogy. The 5-cm-diameter cores were drilled using a diamond core bit and brine as the drilling fluid, with the axis of the core cut parallel to the bedding plane of the interbed layer. The core was cut into three 15- to 24-cm-long cylindrical samples, and tests were performed in a Hassler-type permeability cell using nitrogen as the flowing medium with water providing the confining pressure. Details of the pore- and confining-pressure and other test conditions were not included in the cited report.

The gas permeability tests were performed so that the flow was measured parallel to the bedding plane. According to the report, permeability tests on HPC 1 and HPC 2 yielded permeabilities of 71 and 148 microdarcies, respectively. When a confining pressure of 1200 psi was applied to HPC 1, the permeability decreased to 0.02 microdarcies after 50 hours. When the confining pressure was increased up to 1700 psi, the permeability decreased to 0.002 microdarcies after 246 hours, below the resolution of the test system. Similarly, the permeability of HPC 2 decreased to 1 microdarcy after one day at 1200 psi confining pressure. The third core, HPC 3, which was approximately half the length of HPC 1 and HPC 2, exhibited an initial permeability described only as "high." After 272 hours at 1200 psi confining pressure, the permeability of HPC 3 reduced to 7 microdarcies. It was suggested that the shorter length of HPC 3 contributed to its slower "healing" and resulting higher permeability at similar confining pressure than HPC 1 and HPC 2.

No other laboratory tests to measure flow properties of WIPP-specific Salado anhydrite have been performed.

2.3.3 Field Studies

In situ and laboratory measurements of porosity and permeability (single-phase measurements) are routinely performed for oil and gas reservoir media. Two-phase flow measurements, however, are performed in the laboratory on recovered core samples because two-phase flow measurements are a function of the saturation state of the porous medium, which is difficult to accurately measure in situ.

Saulnier (1992) describes three attempts by NAGRA, Switzerland's national consortium for safe nuclear waste disposal, to determine gas-threshold displacement pressure in situ. A constant pressure test was attempted at the Grimsel Underground Rock Laboratory, and both constant-pressure and constant-rate tests were attempted at Wellenberg. None of the tests was successful because of experiment design and instrumentation limitations.

A test plan to measure gas-threshold pressure in MB 139 at the WIPP was published in March 1992 (Saulnier, 1992), and the initial in situ threshold pressure test is expected to be completed in FY93. The test should result in a capillary pressure measurement. However, because the saturation will not be determined during this in situ test, a laboratory-determined capillary pressure characteristic curve will be necessary to assess whether a true threshold pressure was measured. No other in situ two-phase flow measurements at the WIPP are planned at this time.

3.0 PROGRAM DEFINITION

This section contains the test objectives, program scope, a description of measurement systems under consideration for use, and general program milestones. Additional sections including (1) Experimental Process Description, (2) Instrumentation/Test Equipment/Facilities, (3) Test Requirements, (4) Data Acquisition Plan, and (5) Data Quality Objectives are not contained in this conceptual plan, but will be included in the Test Plan.

3.1 Test Objectives

The Salado Two-Phase Flow Laboratory Program is designed to provide single- and two-phase flow data, characteristic curves, and statistical (distribution) information as well as information regarding appropriate data use to WIPP Program numerical modelers and analysts (Fluid Flow and Transport and Performance Assessment Departments). The program objectives for each fiscal year are described below.

3.1.1 FY92: Determination of Program Needs—Scoping Activities

FY92 was spent performing the following scoping activities:

1. Determine which research efforts require two-phase flow data, how the data is to be used, which rock and flow parameters need to be measured, which rock and flow parameters are required for proper data interpretation, and which stratigraphic units are to be tested.

2. Set priorities for all parameters to be measured and stratigraphic units to be tested.

3. Determine the state of technology development for measuring these parameters and identify and address outstanding programmatic, logistic, or experimental issues.

17

3.1.2 FY93: Determination and Evaluation of Test Methods — Preliminary Experimental Activities

The completion of scoping activities initiated in FY92 and the following preliminary experimental activities will be performed during FY93:

1. Determine the appropriate test methodology for each parameter to be measured (as identified in FY92).

2. Make preliminary measurements of porosity, rock compressibility, single-phase permeability-versus-stress and investigate the use of computed tomography (CT) imaging technology for core damage assessment and tracking fluid flow through cores.

3. Use conventional core analysis techniques to fully characterize samples in terms of mineralogy, composition, and microfractures.

4. Review technical publications and perform preliminary tests to identify potential problem areas.

5. Perform experiments to investigate potential problems identified in the scoping activities.

6. Complete Test Plan.

3.1.3 FY94-FY97: Testing Program — Experimental Activities/Analyses

Using data and information gained from scoping and preliminary experimental activities performed in FY92 and FY93, execute appropriate laboratory tests to provide two-phase flow data, other rock and flow data, characteristic curves, statistics, and other information to WIPP Program numerical modelers and analysts.

3.2 Program Scope

3.2.1 FY92: Determination of Program Needs—Scoping Activities

The FY92 activities described in Section 3.1 are designed to set the groundwork and determine the scope of the Salado Two-Phase Flow Laboratory Program. Figure 4 contains a road map identifying the flow of program activities. As detailed in Figure 4, these activities are intended to answer the following questions:

1. Who is the customer(s) for this work?

2. What rock and flow properties need to be measured?

3. What stratigraphic units/materials should be tested?

4. What are the state-of-the-art technologies, and what is their availability for two-phase flow and other required measurements?

5. Are there any outstanding programmatic, logistic, or experimental issues?

As a result of FY92 activities, WIPP PA numerical modelers, SNL Fluid Flow and Transport numerical modelers and mechanistic model developers, and fluid flow analysts were identified as program customers. The rock and flow properties requested by these customers include porosity, rock compressibility, single-phase permeability, threshold and capillary pressure, and relative permeability. The program customers also identified and set a priority order for the stratigraphic units or other material to be tested: (1) anhydrite interbeds, (2) halite and impure halite, (3) seal material, and (4) backfill material.

Technical discussions were held with Sandia National Laboratories (SNL) scientists and external researchers who have experience in two-phase flow measurements in low-permeability rocks including those from the Institute for Gas Technology (Chicago, IL), the New Mexico Petroleum Recovery Research Center (Socorro, NM), Core Laboratories (Dallas, TX), Golder Associates, US Geological Survey (USGS) (Yucca Mountain), RE/SPEC (Rapid City, SD), Rock Physics Associates (San Jose, CA), and TerraTek (Salt Lake City, UT). An extensive literature review was initiated that covered related topics including core imaging techniques, conventional

19
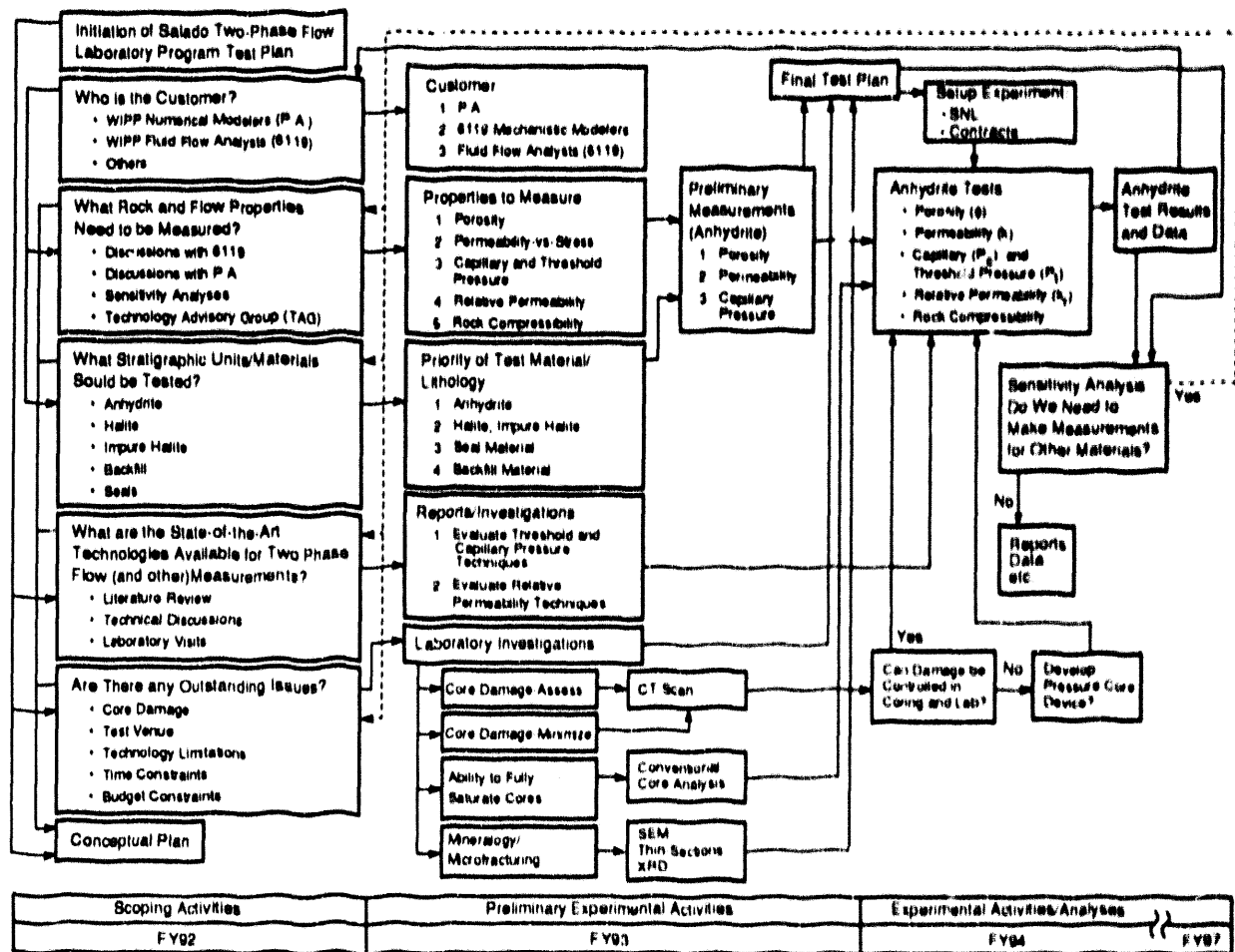
Figure 4. Salado Two-Phase Flow Laboratory Program road map.

and special core analysis, relative permeability measurements, threshold pressure measurements, capillary pressure measurements, and historical research on the Salado Formation anhydrite interbed layers.

A Technology Advisory Group (TAG) was formed consisting of members of SNL's technical staff from the Geoscience and Geotechnology Center who have experience, expertise, or knowledge in relevant areas including natural fractures, core damage, stress state and effective stress, permeability, porosity, capillary pressure, anisotropy, threshold pressure, heterogeneity, and permeability/stress relationships. The TAG meets regularly and provides advice and guidance to the Principal Investigator to address programmatic, logistic, and experimental issues.

3.2.2 FY93: Determination and Evaluation of Test Methods—Preliminary Experimental Activities

Activities planned for FY93 are divided into four areas: (1) laboratory core characterization, (2) preliminary laboratory experiments, (3) reports, and (4) program development. Information gained from FY93 activities will be used to design the long-term two-phase flow laboratory program, remediate problems, evaluate the suitability of using tight gas sands correlations as an analog, and assess our ability to restore specimens to their in situ state.

3.2.2.1 LABORATORY CORE CHARACTERIZATION

There are two objectives of the laboratory core characterization activity. The first objective is to characterize MB 139 because it varies vertically and laterally in composition, and data is needed to correlate variations in transport properties with composition. The second objective is to assess coring-induced damage to MB 139 specimens because damage induced during coring and laboratory subcoring and finishing may affect laboratory porosity and permeability measurements. To meet these goals, core samples from MB 139 will be examined and tested to assess the extent of coring-induced damage (fractures) and characterize lithology,

21

mineralogy, and porosity. In addition, the CT core imaging technique will be tested to evaluate its applicability for identifying and characterizing surface and internal fractures in cores and for tracking fluid flow through Salado anhydrite cores.

MB 139 anhydrite will be tested using techniques including standard petrographic analysis and x-ray powder diffraction. Grain-size distribution and composition will be determined using the petrographic microscope. X-ray diffraction techniques will be used for mineral identification and quantitative compositional analysis.

The extent of surface damage and the crack density will be assessed using epoxy dye-penetrants and CT scanning techniques. Techniques to minimize surface damage, including varying cutting and coring rates, and techniques to remediate surface damage will be investigated. The results of the core-damage assessment experiments will be used to determine whether specialized coring equipment such as pressurized core barrels could reduce coring-induced damage and should be investigated and developed for this application. Also, the results of tests using the CT core imaging technique will be used to make recommendations regarding its applicability in assessing core damage and tracking fluid flow during tests.

3.2.2.2 PRELIMINARY LABORATORY EXPERIMENTS

The objectives of the preliminary laboratory experiments are to measure porosity (total and effective) as a function of stress, measure single-phase permeability under various hydrostatic stress conditions and flow directions, determine the maximum achievable liquid saturation, and perform preliminary capillary pressure measurements. The need for these preliminary measurements is described below:

- Porosity, a fundamental rock property, is a measure of the pore volume within a rock. Porosity has not been measured for the Salado anhydrite material.

22

- Permeability, a measure of the ability of a rock to transmit fluids, has been measured in situ as part of two other test programs and in the laboratory on three poorly described cores (see Section 2.3.3). Because many parameters required for interpretation of the in situ permeability tests have large uncertainty ranges, it will be necessary to measure single-phase permeability in the laboratory under more controlled conditions. In addition, single-phase permeability is required for determining relative permeability.

- Relative permeability and capillary and threshold pressure are defined in terms of the relative saturation of the fluids present in a given porous medium. Single-phase (gas or liquid) permeability and gas threshold pressure measurements require complete saturation of interconnected pore space. Verifying the ability to completely saturate the interconnected pore space of MB 139 specimens will substantiate laboratory tests of both single- and two-phase permeability and threshold pressure.

- As described in Section 3.3.6, there are a number of methods available for measuring capillary pressure in the laboratory. Two methods will be used to measure capillary pressure on a small set of core samples to help determine which method(s) should be used in subsequent tests.

Knowledge gained from this activity will be used to design and implement future tests to measure threshold pressure, capillary pressure, and relative permeability. Additionally, this information will be used to evaluate the suitability of using tight gas sands correlations as a Salado analog and to justify the laboratory approach by assessing the ability to restore specimens to their in situ state.

3.2.2.3 REPORTS

Four reports are planned for FY93 to meet program objectives:

1. "Evaluation of Laboratory Techniques to Measure Relative Permeability for the Salado Formation Anhydrite Interbeds at the Waste Isolation Pilot Plant,"

2. "Evaluation of Experimental Techniques to Measure Threshold Pressure for the Salado Formation Anhydrite Interbeds at the Waste Isolation Pilot Plant,"

3. A report containing the results of core-damage assessment including recommendations for core-damage minimization, and

4. "Salado Two-Phase Flow Laboratory Program Test Plan."

The first two reports will be used to determine the appropriate test methodology for two-phase flow parameters, and the third report will address concerns related to core damage assessment and recommendations for damage minimization. The recommendations from the evaluation of threshold-pressure and relative permeability measurement techniques reports will be used to determine the appropriate methodology for making these measurements and to determine whether such tests should be performed in-house or by contractors. The Test Plan will be an expansion of this conceptual plan and will incorporate recommendations from the two-phase flow method evaluation reports and the results from the core characterization and preliminary laboratory tests.

3.2.2.4 PROGRAM DEVELOPMENT

Technology Advisory Group

The Salado Two-Phase Flow Laboratory Program will continue to evolve and change to meet program demands and needs. The TAG will continue to act in an advisory capacity to address concerns and issues.

Collaborative Program with Gesellschaft fur Reaktorsicherheit and Forschungszentrum Julich

In March 1992, scientists from Gesellschaft fur Reaktorsicherheit (GRS) and Forschungszentrum Julich (KFA) attended the Radioactive Waste Technical Exchange in Albuquerque. At the meeting, a tentative agreement was made for technical exchange and

24

collaborative work in developing techniques to measure two-phase flow properties in salt and anhydrite. As a result, information exchange and coordination meetings were held with these scientists from GRS and KFA in November 1992 in Julich, Germany, to discuss coordination of work on two-phase flow properties. These meetings were intended to formally establish a cooperative program and included technical discussions of the planned WIPP two-phase flow laboratory program, experimental methods, and the need to develop new experimental techniques. During the meetings in Germany, it was acknowledged that the German two-phase flow program was currently unfunded and that when funding is received, their efforts will focus on measuring two-phase flow properties of halite, rather than anhydrite. In light of the GRS and KFA funding situation and area of interest, it was agreed that a cooperative program is not appropriate at this time. However, informal information exchanges between the two programs will continue, and the possibility of developing a collaborative program will be reconsidered in December 1993.

3.2.3 FY94-FY97 Testing Program — Experimental Activities/Analyses

The Salado Two-Phase Flow Laboratory Program is expected to be ready to begin measurements for anhydrite threshold and capillary pressures and relative permeability (gas and liquid) in FY94, as shown in Figure 4. Details of the long-term, two-phase flow test program will be included in the upcoming Test Plan.

3.3 Measurement Systems

The American Petroleum Institute (API, 1960) established standards and guidelines for measuring porosity and intrinsic permeability (single-phase tests) on full-diameter cores and core plugs. These original standards are being updated as a result of technological advances, but as in the original standards, the new guidelines are not expected to include any reference to relative permeability, threshold pressure, or capillary pressure measurements. The SCA recognized this oversight and in 1992 initiated a program to establish guidelines for laboratory measurement of

capillary pressure and relative permeability. As of the publication date of this report, the SCA study is still in progress and relative permeability, capillary pressure, and threshold pressure measurement guidelines have not been published.

Core characterization, core damage assessment, porosity, and single-phase permeability measurements and analyses will follow API or other accepted standards. Because no standards or guidelines exist for measuring relative permeability, capillary pressure, or threshold pressure, test methodology evaluations will be performed during FY93 to determine the appropriate approach for measuring these two-phase parameters. In some cases, more than one measurement technique may be used to accurately quantify these parameters.

As required, all design drawings and material specifications will be made part of the SNL "Quality Assurance Program Description" (QAPD). Details of the measurement systems and analysis will be found in the evaluation reports (see Section 4.2.2) and Test Plan, but a general discussion of measurement systems for the two-phase flow tests is found in this section.

3.3.1 Core Characterization

The composition of MB 139 varies in the lateral and vertical directions, and data are needed to correlate variations in flow properties with composition. MB 139 core samples will be examined and tested on a microscopic scale to assess the extent of coring-induced damage (fractures) and characterize lithology, mineralogy, and porosity using standard petrographic analysis techniques as described by Basan et al. (1988). Thin-section analysis will be used to identify matrix, detrital, cement, and pore composition and define the nature (type and distribution) of porosity. X-ray diffraction (XRD), which can account for components too small to be identified using light microscopy (LM) techniques, will be used to identify and quantify bulk rock and clay mineralogies. In addition, scanning electron microscopy (SEM) will be used to determine the morphology and location of clays, qualitatively evaluate pore geometry, and further define porosity.

3.3.2 Core Damage Assessment

Damage in the form of microfractures may be induced during drill coring, laboratory subcoring, and finishing operations on recovered rock specimens. Core damage may affect laboratory measurements of porosity, capillary and threshold pressure, and permeability, and unless the core can be restored to its in situ state, laboratory-derived parameters may not be representative of the Salado far-field. In addition to the microscopic core characterization tests previously described, two macroscopic techniques (standard epoxy dye-penetrant impregnation techniques, and CT imaging) will be applied during the preliminary core analysis in FY93 to evaluate their effectiveness for damage detection and quantification in MB 139 cores. Techniques to minimize surface damage, including varying cutting and coring rates, and techniques to remediate surface damage will also be investigated. Other techniques, such as acoustic wave velocity and resistivity measurements, may be used to determine the relationships between stress state, damage, and permeability.

The results of the core-damage assessment experiments will be used to determine whether specialized coring equipment could effectively reduce coring-induced damage and should be investigated and developed for this application. Also, the results of tests using the CT core imaging technique will be used to make recommendations regarding its applicability in assessing core damage and tracking fluid flow during tests.

3.3.2.1 EPOXY DYE-PENETRANT IMPREGNATION

Standard epoxy dye-penetrant impregnation is intended to provide macroscopic quantitative information and qualitative visual illustration of coring-induced damage effects. In this simple technique, the outer surface of a cylindrical core sample is injected with an epoxy dye-penetrant while under pressure. The epoxy-dye mixture then flows into the core through surface or internal fractures. The epoxy is allowed to cure, then the epoxy-coated core is removed from its container and cut in half longitudinally as shown in Figure 5. Coring-induced damage is quantified by comparing the outer core surface with the inner material by counting fractures that

27
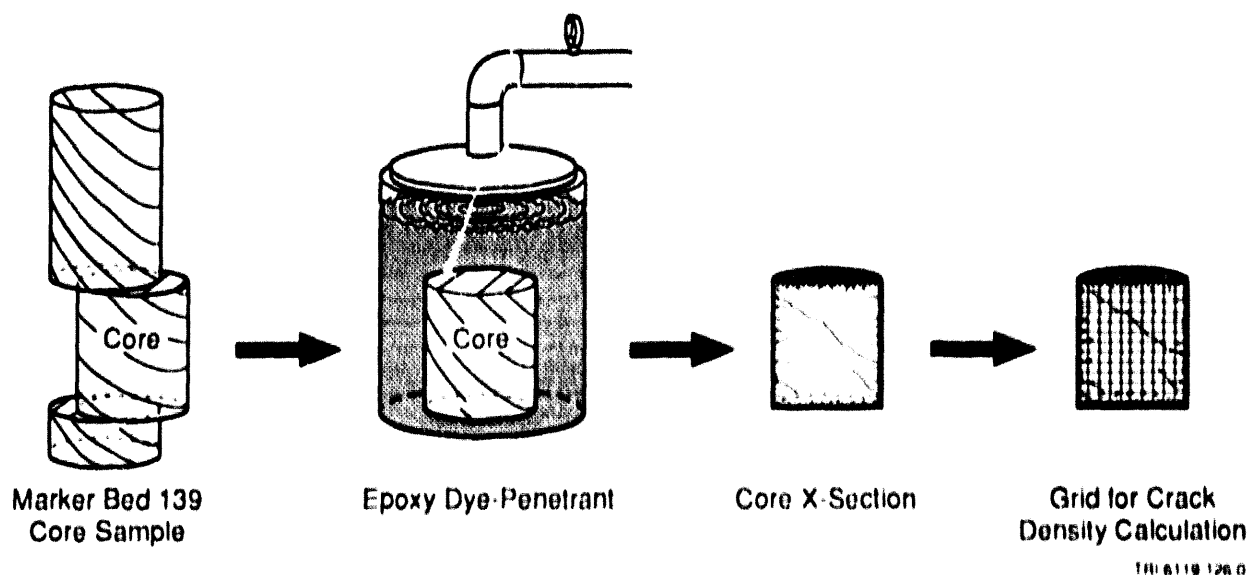
Figure 5. Epoxy dye-penetration.

cross lines on an overlain grid. Crack density adjacent to the field-cored surface and at the sample center are determined, using standard stereological procedures.

3.3.2.2 COMPUTED TOMOGRAPHY

CT imaging will be evaluated as a tool for identifying and characterizing surface and internal fractures and for tracking fluid flow through MB 139 cores. CT is a powerful tool for evaluation of coring induced damage at scales varying from pore to whole core, measurement of core-scale heterogeneity and fluid saturation distribution, and investigation of the mechanisms that govern the response of geomaterial to stress. CT may prove useful for assessing the overall condition of whole cores, selecting core plug locations and the number required for complete core characterization, and providing insight into reducing coring induced damage.

CT, more commonly known as CAT (computer-aided tomography) scanning, was originally developed for the medical industry. It is a nondestructive analytical tool that uses x-rays to evaluate the internal structure of an object. The CT scanner consists of a rotating x-ray source and detector that encircles a core positioned horizontally upon a gantry table. The core is

advanced through the apparatus and scanned at fixed increments. Computer software reconstructs two-dimensional images (or slices) in the plane of an x-ray beam directed through the object at many different angles. A series of the two-dimensional images is used to show three-dimensional features within an object.

Good agreement exists between CT-determined porosity and porosity determined from standard petrography and core analysis for oil field cores. CT imaging will be evaluated in FY93 for use in identifying and characterizing surface and internal fractures. As illustrated in Figure 6, a whole-core scan will be performed on a 1.5-m-long vertical section of core drilled through MB 139 to detect coring-induced surface fractures and natural or coring-induced internal fracture. After the initial scan, the whole-core will be sub-cored to produce smaller plug-size
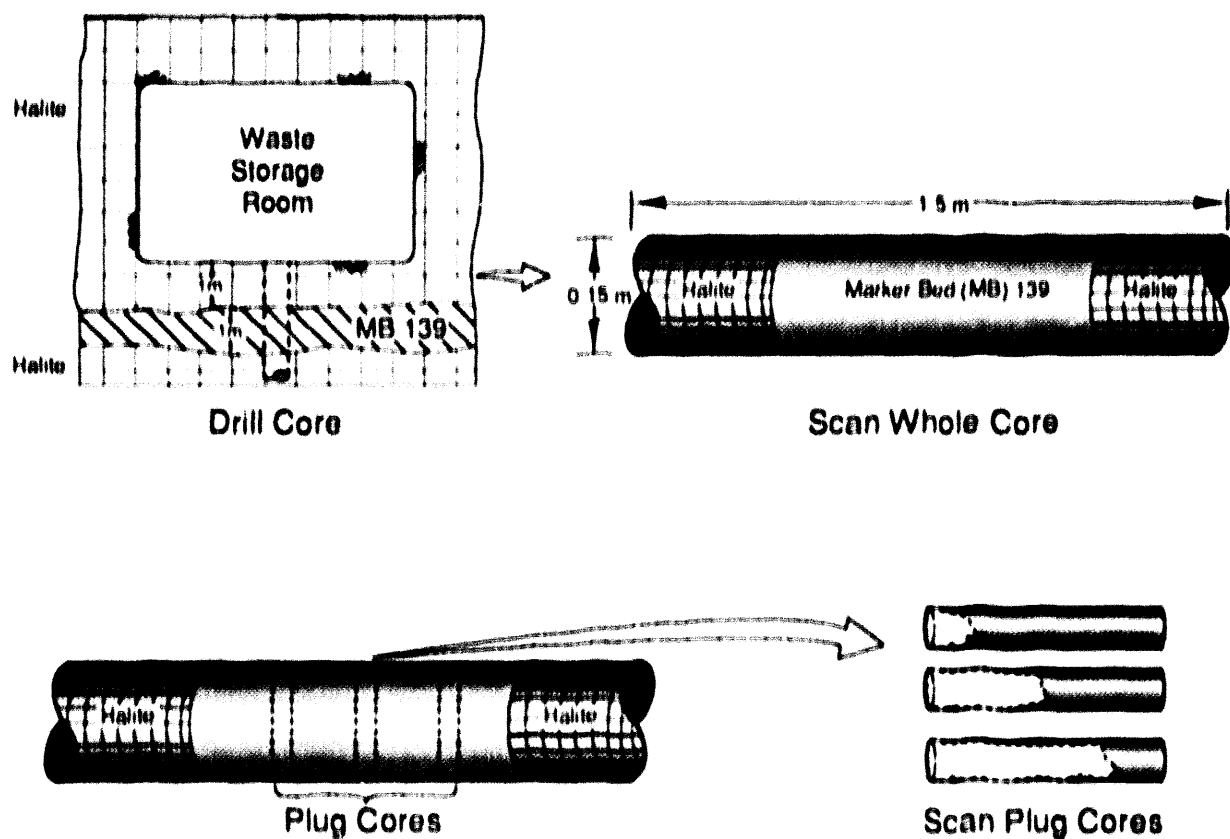
Figure 6. CT scanning of MB 139 cores.

cores. The plug cores will then be scanned while dry and during a fluid flow test to detect any new laboratory-coring-induced or finishing-induced fractures.

3.3.3 Porosity

Porosity is a measure of the void space or storage capacity of a rock and is quantified as the ratio of void (pore) volume of a rock sample to its total or bulk volume (grain volume plus pore volume). Determination of porosity, ϕ, requires solution of Equations 6 and 7 and measurement of two of the following three variables: pore volume (V_p), grain volume (V_g), and bulk volume (V_b).

$$\phi = V_p / V_b \tag{6}$$

$$V_b = V_p + V_g \tag{7}$$

Choice of porosity measurement technique depends upon the type of rock, time available, and whether one seeks to measure total or effective porosity. Total porosity is calculated using the total pore volume of the sample, whereas effective porosity is calculated using only the interconnected pore volume of the sample. The difference between total and effective porosity may be negligible for permeable, high-porosity rocks but may be significant for tight, low-porosity rocks where the pores are not well-connected. In general, effective porosity is measured on intact rock samples, and total porosity measurements require crushing the sample. Details of the following techniques for measuring pore, grain, and bulk volumes are found in the *Recommended Practice for Rock Core-Analysis Procedure* (API, 1960).

3.3.3.1 PORE VOLUME (V_p)

Pore volume can be measured directly by resaturating the void space of a clean, dry core by one of two methods: 1) evacuating and saturating with liquid, or 2) saturating the nonevacuated

pore space with helium or other gas. Because liquids may drain from large surface pores, the liquid saturation method is not suitable for vuggy samples. However, if proper precautions are taken (i.e., the core is wrapped with a screen and contained within a rubber sleeve—the screen prevents the rubber sleeve from extruding into surface vugs—and confining pressure is applied to seal surfaces of the sample), the gas saturation method can be used. The gas saturation technique, which applies Boyle's law, is an excellent method especially when helium is used. Helium molecules are small, they rapidly penetrate into tiny pores, and because helium is inert, it is not adsorbed on rock surfaces as air might be (Keelan, 1972).

3.3.3.2 BULK VOLUME (V_B)

Bulk volume can be determined a number of ways including calipered length measurements, use of a calibrated mercury pump (porosimeter), or application of Archimedes principle. Because none of these standard methods is designed to be performed under overburden stress conditions, errors can be introduced if the rock compacts significantly at overburden stress.

In the caliper method, core dimension is measured with a caliper and appropriate mathematical formulae are applied to calculate the bulk volume. This technique is simple and does not require sophisticated equipment, but it is not applicable to irregularly shaped cores (i.e., nonright cylinders) because valid average dimensions cannot be determined.

Bulk volumes of small plugs can be determined using a calibrated mercury pump, also known as a mercury porosimeter. In this method, the bulk volume is calculated in the following manner: 1) the volume of a chamber (V_{c1}) is determined by filling it with mercury, 2) mercury is drained from the chamber, 3) the core sample is placed in the chamber, 4) the chamber (with core in place) is refilled with mercury (V_{c2}). The bulk volume is then calculated by subtracting V_{c2} from V_{c1}, as shown in Equation 8.

$$V_b = V_{c1} - V_{c2} \ .$$
(8)

31

This method is not applicable for rocks with surface pores because mercury may penetrate surface vugs or pores and the bulk volume of the samples would be underestimated.

Archimede's principle is applied to measure bulk volume using mercury as described in Basan et al. (1988): (1) a core sample is cleaned, dried and weighed, (2) a beaker of mercury is weighed (W_{Hg}), (3) the core is submerged in the mercury-filled beaker, and (4) the core in the mercury-filled beaker is reweighed ($W_{Hg+core}$). Bulk volume is calculated as described in Equation 9, where ρ_{Hg} is the density of mercury.

$$V_b = [W_{Hg+core} - W_{Hg}] / \rho_{Hg} \quad .\qquad (9)$$

Although less toxic fluids can be used, mercury is a nearly perfect nonwetting fluid because it will not enter the pore space. Error in this and the porosimeter methods can be introduced by the development of a hydraulic head as the rock is immersed in mercury. Studies show that the most reliable procedure is to submerge the sample under less than 4 mm of mercury (Basan et al., 1988).

3.3.3.3 GRAIN VOLUME (V_G)

The Boyle's law double-cell porosimeter is the most widely used device for determining grain volume. In the method outlined by Basan et al. (1988), the core is placed in a sample chamber that is connected by a valve to a reference chamber, where a transducer measures pressure. The reference chamber is initially isolated from the sample chamber and filled with gas, often helium, to a reference pressure. The connecting valve is then opened to allow the helium pressure to equilibrate between the two chambers, and the final pressure is a function of the grain volume. This quick technique is valid on clean and dry samples. Grain volume in whole cores may also be calculated using measured sample weight and knowledge of average grain density, but this method is not applicable for heterogeneous rocks.

Two other methods, summation-of-fluids and resaturation, are also used to determine porosity directly, but are better suited to high porosity/high permeability (i.e., oil reservoir rocks). According to Basan et al. (1988), summation-of-fluids uses a retort to drive off and recover fluids (oil, water, and/or gas) from a crushed core. The volume of each recovered fluid is determined, and, on another crushed core sample, the bulk and void volumes are determined by mercury displacement and injection, respectively. Porosity is calculated by dividing the sum of the recovered fluid volume by the bulk volume. Error may be introduced because two different cores are used and, because some of the fluid may remain in the rock, low porosity measurements may result, especially in tight rocks. In the restoration method, bulk and pore volumes are obtained by comparing the weight of a clean dry core with that of the same core saturated with a fluid of known density. This technique should not be used in vuggy carbonates because fluids may be lost from the surface during weighing. Also, because the core is saturated in a vacuum, when the sample is returned to atmospheric pressure for weighing, the fluid draining from the core may carry grains away.

Total and effective porosity will be measured for MB 139 core samples as part of the preliminary tests scheduled for FY93. Information on the specific measurement systems is not available at this time, but will be included in the Test Plan.

3.3.4 Permeability

Permeability is a measure of the ability of a porous medium to transmit fluid. Permeability measurements can be made in the laboratory using steady-state or unsteady-state techniques. Using standard steady-state laboratory equipment developed for the oil and gas industry, measurements of absolute permeability (also referred to as intrinsic or single-phase permeability) ranging from 10^{16} to 2×10^{11} m^2 (approximately 1×10^{4} to 20 darcys) can be made on full diameter and plug-size cores (Keelan, 1972). Specialized techniques incorporating unsteady-state or transient techniques were developed for the underground gas storage industry and yield measurements as low as 10^{21} m^2 (10^{9} darcys).

3.3.4.1 STEADY-STATE METHODS

Steady-state permeability is determined in the laboratory by measuring the flow rate and pressure differential across a shaped core while a fluid is passed through the core. This technique is valid if laminar flow conditions exist (i.e., flow rate is proportional to the pressure gradient) and if no reaction occurs between the rock and flowing fluid. Standard procedures for measuring single-phase permeability are described in API RP27 and API RP40 (API, 1956; 1960), which also include schematic diagrams and equations for calculating permeability for specific test conditions. Steady-state methods are slow, especially for low permeability rocks.

Dry gas is the standard fluid used in permeability measurements because it is non-reactive with rock and easy to use, but non-reactive liquids are also applicable. Steady-state permeability is determined by placing a clean dry core of known dimensions into a chamber, or permeameter, and flowing gas or liquid through the core while measuring the pressure difference across the core and the gas or liquid flow rate. Generalized equations for calculating permeability on a core cut as a right-circular cylinder under laminar flow conditions are presented below as Equations 10a and 10b for gas and liquid, respectively.

$$k_g = \frac{2 Q_o P_o L \mu_g}{(p_i^2 - p_o^2) A} \tag{10a}$$

$$k_l = \frac{Q_o L \mu_l}{(P_i - P_o) A} \tag{10b}$$

where

k_g = gas permeability
k_l = liquid permeability
Q_o = gas flow rate at outlet end
P_o = outlet pressure (often equal to atmospheric pressure)
P_i = inlet pressure
μ_g = gas viscosity
μ_l = liquid viscosity
L = length of core
A = cross-sectional area of core, perpendicular to direction of flow.

(Note that permeability can be measured in the laboratory under turbulent flow conditions using several different flow rates and Forscheimer's equation.)

Differences between gas and liquid permeabilities measured in the laboratory are noted in the literature and are generally attributed to the Klinkenberg, or gas slippage, effect (i.e., gas has higher velocity near a grain surface than a liquid, see below). Likewise, differences between in situ and laboratory measured permeability for either gas or liquid may be attributed to the absence of sufficient confining stress on the core during laboratory measurements.

Klinkenberg Effect

Klinkenberg (1941) investigated gas flow through porous media and found variations in the measured permeabilities depending upon the gas or nonreactive liquid used and the mean pressure, P_m, existing in the core during the test. The differences in gas permeabilities were attributed to gas slippage, which occurs when the diameter of the pores approaches the mean free path of the gas. As expected, low permeability rocks are more sensitive to the Klinkenberg effect than high-permeability rocks (Keelan, 1972).

As shown in Figure 7, in a plot of gas permeability versus the reciprocal of the mean pressure, a straight line is formed for each gas that can be extrapolated to a single infinite mean
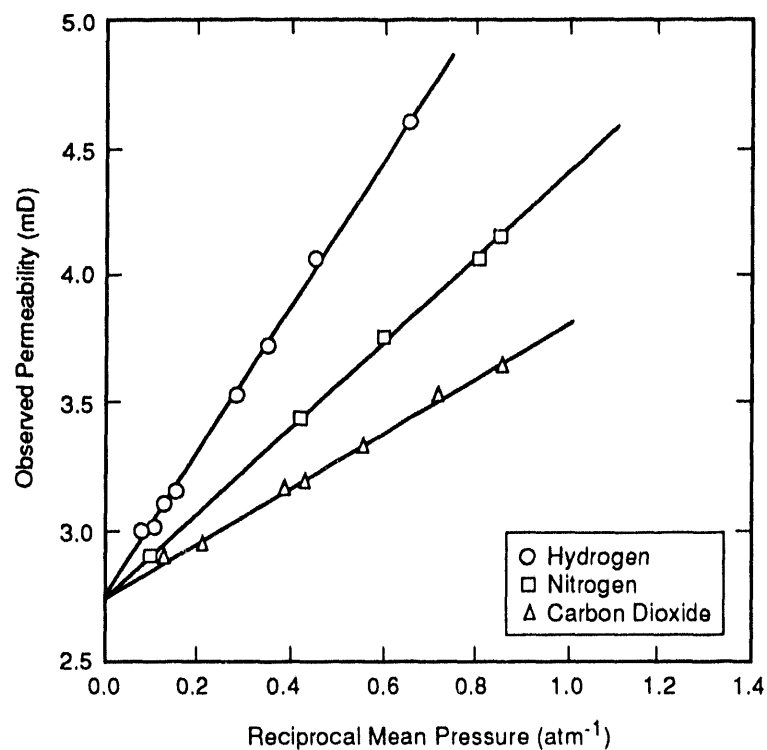
TRI-6119-127-0

Figure 7. Permeability versus reciprocal mean pressure (after Klinkenberg, 1941).

pressure value. This extrapolated mean pressure corresponds to a permeability, k_l, that is comparable to a permeability measured for a core fully saturated with a nonreactive liquid. The relationship between measured gas permeability and equivalent liquid permeability, k_g and k_l, respectively, is expressed in Equation 11.

$$k_g = k_l \left(1 + b / P_m\right) \qquad (11)$$

where

P_m = the mean flowing pressure (absolute) of the gas during the test

k_l = the value of permeability corresponding to infinite mean pressure and liquid permeability

k_g = the value of permeability for a gas at P_m

36

b   =   a rock- and gas-specific constant that depends upon the mean free path of the gas and the pore structure of the rock and varies inversely with the average pore radius.

Correlations are available that relate the laboratory-measured air permeabilities to equivalent liquid permeabilities. These correlations yield values of sufficient accuracy for sandstones and some limestones, but are not applicable to whole core permeability measurements because of the larger degree of heterogeneity.

3.3.4.2 UNSTEADY-STATE METHODS

Unsteady-state methods, including pulse decay (Freeman and Bush, 1983) and pressure transient (Hseih et al., 1981), are used for measuring hydraulic properties of low permeability core samples in the laboratory. These methods use pressure transient analysis to infer permeability.

Pulse-Decay

This transient flow method was introduced by Brace et al. (1968) to measure the permeability of Westerly Granite. In this method, a cylindrical core sample is connected to two fluid reservoirs—one on the upstream end and the other on the downstream end of the core—each initially at the same pressure. The experiment is initiated by suddenly increasing, or pulsing, the pressure in the upstream end of the core causing the fluid to flow through the core to the downstream reservoir. The pressure decay in the upstream end of the core is monitored, and the permeability is calculated from the pressure decay versus time data. This method can be performed at simulated in situ stress conditions.

Pressure Transient

As described by Freeman and Bush (1983), the sample is also connected to two reservoirs in this method; however, the downstream reservoir volume is approximately the same

as the sample pore volume. A gas is introduced into the upstream end of the sample at a pressure greater than atmospheric, but well below the sample's external confining pressure. As the gas flows through the sample, the pressure in the small-volume downstream reservoir is monitored as it increases. Permeability is then calculated from the pressure buildup data used to determine the flow rate out of the sample. This method can be performed at simulated in situ stress conditions.

3.3.4.3 EFFECTS OF STRESS ON PERMEABILITY

Differences between in situ and laboratory measured permeability for either gas or liquid may be attributed to differences in, or the absence of, sufficient confining stress on the core during laboratory measurements. Tests show that laboratory-measured single-phase permeability is significantly reduced when confining pressure is applied to cores during permeability tests (Fatt and Davis, 1952; Gray et al., 1963). Jones and Owens (1980) noted that for their Tight Gas Sands core samples, permeability was reduced by an order of magnitude when hydrostatic confining pressure equal to a net overburden pressure was applied. Further, their findings agreed with McLatchie et al. (1958) and showed that, in general, the lower the core permeability, the more it is affected by confining pressure. (The effects of stress and the concept of effective stress are addressed in Section 3.3.7.)

Single-phase permeability measurements planned for FY93 as part of the preliminary MB 139 tests will include both gas and liquid (brine and non-reactive mineral spirits) permeability tests. The brine permeability tests will be designed to allow for sampling of the brine prior to entering the core and after flowing through the core, and the brine composition will be analyzed to determine if the brine is reacting with the core material. These gas and liquid permeability tests will be configured so that the flow direction is parallel to the bedding plane. Another set of gas permeability tests will be performed with permeability measurements made perpendicular to the bedding plane. These tests will help determine the magnitude of permeability anisotropy in MB 139. The gas permeability measurements will be corrected for Klinkenberg effects. All

permeability tests will be performed under net effective stress conditions to simulate in situ stress conditions.

3.3.5 Capillary and Threshold Pressure

Several WIPP numerical modelers requested measurement of gas threshold displacement pressure and capillary pressure for the Salado anhydrite interbeds. Gas threshold pressure, as described below, is actually a point on a capillary pressure characteristic curve, and can be measured directly or in conjunction with capillary pressure curves. It is intended, within the scope of this program, to measure capillary pressure characteristic curves over a complete saturation range, thus providing both threshold pressure and capillary pressure data and independent measurement of threshold pressure.

Gas threshold displacement pressure is the pressure that the gas (nonwetting phase) must reach to overcome the pore pressure and capillary effects (threshold pressure) to enter a porous media and displace the wetting-phase fluid. Capillary effects are quantified as capillary (P_c) or threshold pressure (P_t). Threshold pressure is related to the capillary pressure characteristic curve as shown in Figure 2 and is defined as either: 1) the endpoint pressure on the capillary pressure-versus-saturation curve corresponding to a wetting-phase saturation of 1.0, or 2) the pressure on the capillary pressure-versus-saturation curve at the nonwetting-phase critical saturation. The first definition applies to the initial penetration of the nonwetting phase fluid into the wetting-phase saturated porous medium, and the second applies to the development of a nonwetting phase continuum through the core and initial breakthrough for the nonwetting-phase fluid.

3.3.5.1 DIRECT LABORATORY MEASUREMENT OF THRESHOLD PRESSURE

Direct methods for measuring threshold pressure in the laboratory include the pressure leveling technique, constant rate technique (Rudd, 1974), and the pressure-step method described by Thomas et al. (1968). Historically, the natural gas storage industry was interested in

39

determining the threshold pressure of low-permeability media, and most of the direct threshold pressure measurement techniques were developed to support gas storage technology.

Constant-Rate Technique

Constant-rate injection techniques are used to determine threshold pressure independent of capillary pressure. A known quantity of gas is introduced into a brine-saturated core at a very low constant rate. Pressure is recorded at the inflow face as the pressure increases. When the threshold pressure is reached, the slope of the pressure buildup curve decreases or reverses as gas enters the sample (Rudd, 1974).

Pressure Leveling Technique

The pressure leveling technique was developed from a constant rate test to overcome some of the problems inherent to the pressure-step technique: a fixed volume of gas at a known pressure (greater than the expected threshold pressure) is applied at the input end of a core. The gas expands into the core until it equilibrates or "levels" with the threshold pressure. Rudd (1974) compared results from this method with threshold pressure measured using the pressure-step method and found good agreement. Where discrepancies did exist, he found the pressure leveling technique to be more valid.

Rudd also applied this technique sequentially to the same core sample, and as expected, found that the threshold pressure is dependent upon the specific surface encountered within a core, usually at or very near the gas-input end of the core. He recommends applying the technique at a minimum of two zones in a single core.

Compressibility and gas diffusion problems can be factors in this technique when gas is used as the nonwetting phase fluid. However, because the gas pressure is monitored throughout the test, equilibration is readily observed and test time is significantly reduced.

40

The pressure-step method has been used for the past 30 years to measure threshold pressure in the laboratory. This method consists of introducing gas into the end of a brine-saturated core, allowing the core/gas/brine system to equilibrate, and observing the outflow end of the core to detect the first fluid movement from the core. The gas pressure is increased incrementally until fluid flows from the core. There are two significant problems with this method: (1) long equilibration times, and (2) compressibility of the gas, brine, rock, and experimental apparatus. Equilibration time at each pressure step can range from hours to days, depending upon the permeability of the sample. Compressibility of the gas and brine can also be a problem because the initial input of gas into the pore is accommodated by compression of the gas and brine until it can be bled off through the whole core (Rudd, 1974). Because this must be repeated at every pressure step, this method is very time-consuming. The length of time required for these tests adds experimental complications such as continuously maintaining constant pressure for days and preventing minute gas leaks. Another problem that may be encountered is gas diffusing into the brine, which may be mitigated by saturating the gas with water.

3.3.5.2 INDIRECT LABORATORY MEASUREMENT OF THRESHOLD PRESSURE

Threshold pressure is obtained indirectly from capillary-pressure characteristic curves. The capillary pressure curve also provides data on the irreducible wetting-phase saturation that is crucial for defining effective saturation for both the Brooks and Corey (1964) and Parker et al. (1987) correlations. Threshold pressure is determined by extrapolating or interpolating the capillary pressure curve to the appropriate saturation value of either 100% wetting phase (brine) saturation or critical nonwetting phase (gas) saturation as shown in Figure 2. Using the indirect methods for determining threshold pressure is advantageous because these methods provide the entire capillary pressure curve, which is necessary for justifying the use of the Brooks and Corey (1964) and/or Parker et al. (1987) correlations in the PA models.

Capillary pressure, P_c, is the pressure difference across an interface between two immiscible fluids as described in Equation 12.

$$P_c = P_{nw} - P_w = \sigma \left(\frac{1}{r_1} - \frac{1}{r_2} \right)$$ (12)

where

P_{nw}	=	pressure of the nonwetting phase
P_w	=	pressure in the wetting phase
σ	=	interfacial tension
r_1, r_2	=	principal radii of curvature of a point on the interface.

Laboratory techniques to measure capillary pressure are divided into static or dynamic (time-dependent) methods. The static methods discussed in this section include the porous plate, centrifuge, and the mercury injection methods. In addition, one dynamic method is also discussed.

Porous Plate

As described by Bass (1987) and shown in Figure 8, the porous plate, or porous diaphragm, method requires a permeable membrane that contains a uniform pore size distribution. The pore size distribution is selected so that the displacing fluid will not penetrate the membrane when the applied pressure is below a selected value. Pressure is applied across the membrane, made of materials such as fritted glass or cellophane, and is increased in small increments. The core is allowed to stabilize at each pressure step where the saturation of the core is calculated. This method has the advantage that any combination of fluids may be used and both drainage and imbibition curves can be obtained, but it is time-consuming because of long equilibration times and may take several weeks to complete an entire capillary pressure curve. Fluid distribution throughout the sample is probably not uniform at any time.

42
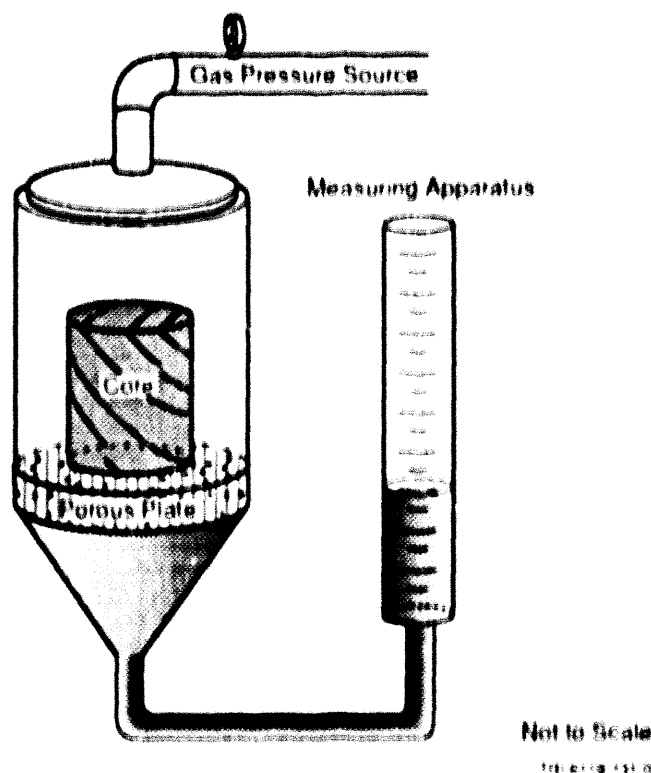
Figure 8. Schematic of porous plate method of capillary pressure (Bass, 1987).

Centrifuge

The centrifuge method is nondestructive, yields reproducible results, and can provide data for both drainage and imbibition curves. During a drainage test (nonwetting phase [gas] displacing the wetting phase [brine]) a core is fully saturated with brine and placed on a water wet semipermeable membrane inside a core holder in a centrifuge rotor. A low rotation rate is selected and the core is spun. The high acceleration rate increases the force field on the fluids and, in effect, subjects the core to an increased gravitational field (Bass, 1987). The volume of brine is measured as the core is rotated until the volume of expelled brine is constant. An average value of brine saturation is calculated for the core for that rotation rate, and the rotation speed is converted into force units in the center of the sample. A higher rotation rate is selected and steps are repeated.

In addition to being very fast, the centrifuge method has several advantages: it provides good correlation with the porous plate method, it can accommodate up to 1000-psi pressure differential between phases in an air/liquid system, it can be used for time-dependent saturation measurements and 2- and 3-phase relative permeability testing, and it can mitigate capillary-end effects and viscous instability of gas displacing liquid. However, fluid distribution throughout the sample may not be uniform.

Mercury Injection

In the mercury injection method, a core sample is inserted into a mercury chamber and evacuated. Volumes of mercury, a nonwetting fluid, are then incrementally forced into the core under pressure. The volume of mercury injected at each pressure is used to determine the nonwetting-phase saturation, and the process is repeated until the whole capillary pressure curve is obtained (Bass, 1987). This is a destructive method for determining capillary pressure, and because an air-mercury system is used, interpretation and direct application to other rock and fluid systems may be difficult. One must also convert the mercury surface-tension behavior to that of the fluids in the reservoir.

Dynamic

In dynamic capillary pressure tests, capillary pressure is determined by establishing simultaneous steady-state two-phase flow in a core sample. As described by Bass (1987), special wetted disks are used that permit hydraulic pressure transmission of only one phase, and capillary pressure is calculated as the difference in the two fluid pressures. The fluid saturations are varied by regulating the volume of the fluids at the inlet end. A complete capillary pressure curve is obtained using this method.

A detailed investigative study, including capillary pressure scoping experiments using the centrifuge and mercury injection methods, will be made in FY93 to determine the most appropriate method(s) to use for determining threshold and capillary pressures of MB 139 core

samples. As part of the FY93 Experimental Scoping Activities, preliminary laboratory tests are planned using the mercury injection and centrifuge methods to assess their applicability in this program. The results of this study will be included in the Test Plan.

3.3.6 Relative Permeability

Whereas intrinsic or absolute permeability is a measure of the ease with which a single fluid will flow through a porous medium, relative permeability compares the ease with which a fluid will flow through a porous medium when another fluid is present. When two fluids flow through a porous medium simultaneously, each fluid has its own effective permeability, and the sum of the two effective permeabilities is always less than the intrinsic or absolute permeability. Relative permeability for wetting and nonwetting phases is described in Equations 13 and 14, and a plots of relative permeability is shown in Figure 9.

$$k_{r_{nw}}(S_w) = \frac{k_{nw}(S_w)}{k} \qquad (13)$$

where

$$k_{r_v}(S_w) = \frac{k_w(S_w)}{k} \qquad (14)$$

k	=	Absolute or intrinsic permeability
$k_{nw}(S_w)$	=	Effective permeability of nonwetting phase at saturation S_w
$k_w(S_w)$	=	Effective permeability of wetting phase at saturation S_w
$k_{rnw}(S_w)$	=	Relative permeability of nonwetting phase at saturation S_w
$k_{rw}(S_w)$	=	Relative permeability of wetting phase at saturation S_w.

45
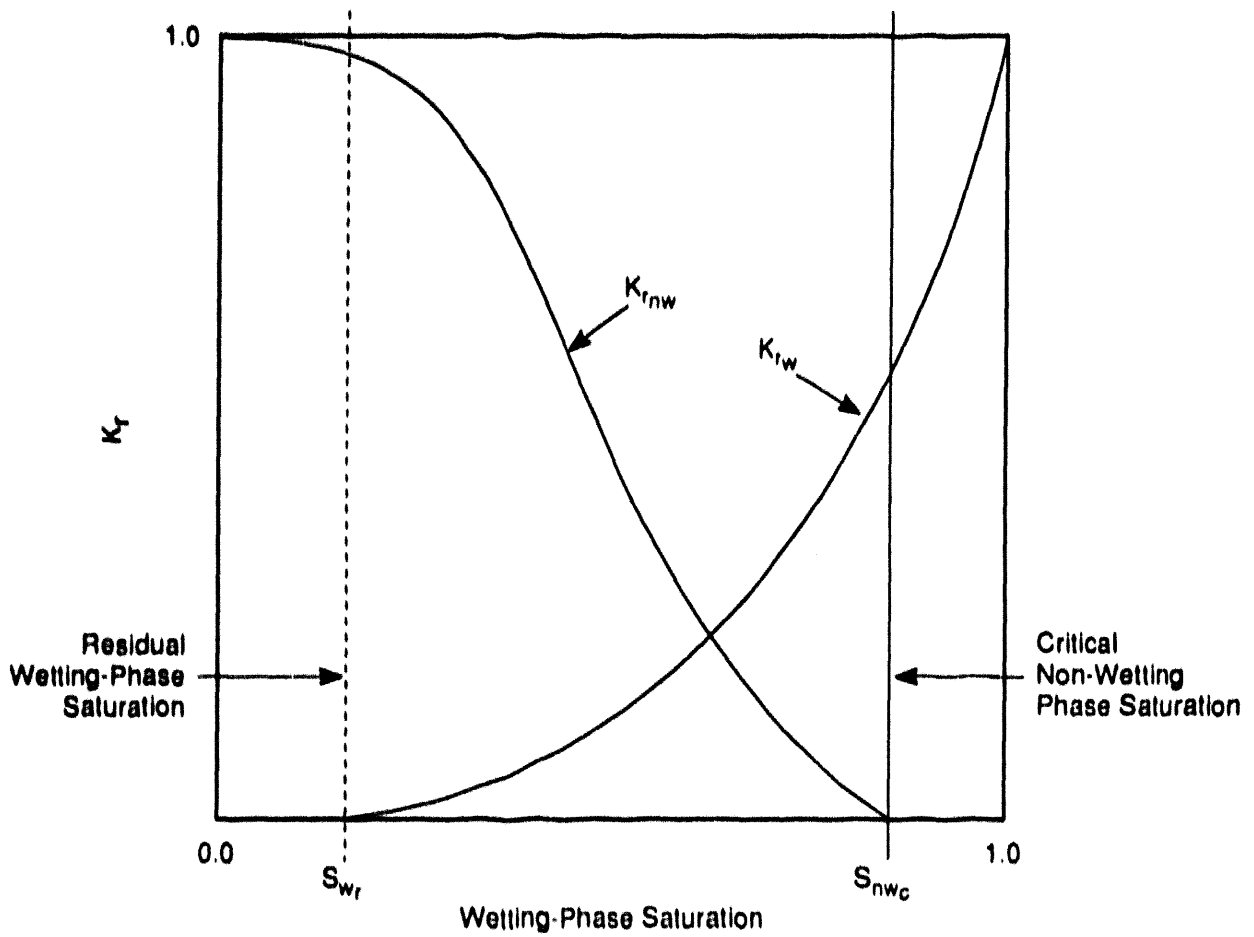
Figure 9. Relative permeability as a function of saturation.

TRI 6119-129-0

Techniques used to measure relative permeability fall into one of two categories: steady-state tests and unsteady-state or transient tests. Unsteady-state tests are more common, requiring less time than steady-state tests, but the debate continues as to which technique better reflects in situ flow conditions (Basan et al., 1988).

3.3.6.1 STEADY-STATE METHODS

In steady-state measurements of relative permeability, effective permeability is calculated as a function of saturation, and calculations are based upon the assumption that Equations 13 and 14 correctly model two-phase flow. Direct measurements are then required of volumetric flow rates, pressure differences across the core sample, and saturation levels. Steady-state methods are slow because time is required for the fluids to equilibrate in the rock at each saturation point, typically taking a few days to weeks, depending upon the permeability. The literature refers to a number of techniques for making steady-state relative permeability measurements including the Hassler method, Penn State method, Hafford method, and dispersed-feed method. Basically, each of these techniques depends upon the same flow mechanism, and they differ only in the way fluid is introduced into the core and in the way adjustments are made for end effects.

End effects arise from a saturation discontinuity existing at the outflow face of the core because the fluids flowing through the core are discharged into a region void of the porous medium. At the outflow face, all the fluids exist at the same pressure; whereas immediately within the pores of the rock at the outflow face, capillary pressure conditions require that the saturation of the wetting phase approach 100% and a saturation gradient is established in the wetting phase of the flow system (Amyx et al., 1960).

Steady-state measurements typically follow these steps to obtain a drainage or desaturation curve (Amyx et al., 1960): 1) a core sample is selected, finished, fully saturated with the wetting-phase fluid, and mounted in a core holder or rubber sleeve; 2) the test cell is prepared, and the ends of the core sample are connected to appropriate porous disks or other devices to minimize end effects; 3) the two fluids are introduced at the inlet end through separate

47

systems at a predetermined ratio; 4) the fluids are flowed through the core until the produced fluid ratio equals the inlet fluid ratio; 5) the core system is considered to be in steady-state flow, and the saturations are measured and relative permeability calculated for that saturation point; 6) the inlet fluid ratio is increased as more of the wetting-phase fluid is removed until steady-state conditions are reached. These steps are repeated until the entire relative permeability curve is obtained. An imbibition curve can also be obtained by initially saturating the core with the nonwetting-phase fluid, and the inlet fluid ratios begin with high nonwetting-phase values and end with high wetting-phase values.

Saturations are measured either internally or externally in a variety of fashions. External methods include measurement of core resistivity, removal of core from test cell for weight measurement, and a volumetric balance of all fluids injected and produced from the sample. The saturation can be measured internally using x-ray or radioactive tracer scans.

3.3.6.2 UNSTEADY-STATE METHODS

According to Rose (1987), in unsteady-state relative permeability tests, the idea is to observe the cumulative production from controlled two-phase flow experiments and then back-calculate relative permeability values that are consistent with the observed outcomes. This lack of certainty in interpretation of these indirect measurements is offset by the small amount of time required for the tests and the corresponding lower cost. Unsteady-state tests can be performed rapidly on small core samples with only a small amount of equipment.

In unsteady-state measurements, a core sample is selected, finished, fully saturated with the wetting-phase fluid, and mounted in a core holder or rubber sleeve. Then gas or other displacement fluid is injected into the core and outlet end fluid volumes are recorded. Relative permeability is calculated using mathematical models usually based upon the Buckley-Leverett equation and saturation is calculated using the cumulative production values. The Buckley-Leverett equation does not apply until the displacement fluid is produced at the outflow end of the core. According to Amyx et al. (1960), end effects are not important when gas is the

displacement fluid because of the high pressure drops involved. The magnitude of capillary-pressure end effects is extremely small compared with the imposed flow gradient, so that the equipment required to counteract end effects is unnecessary. In addition, the test time is short, so all effects of gravitational forces can be neglected. If the condition of negligible capillary pressure and gravity effects is satisfied, the only measurements required are cumulative fluid injected and produced as a function of time.

Steady-state and unsteady-state relative permeability measurements do not always agree: many steady-state measurements show little or no hysteresis in the wetting-phase wettability, whereas large amounts of hysteresis occur in unsteady-state measurements (Basan et al., 1988). A detailed investigative study will be made in FY93 to determine the most appropriate method(s) to use for determining relative permeability of MB 139. The results of this study will be included in the Test Plan.

3.3.7 Rock Compressibility and Effective Stress

3.3.7.1 ROCK COMPRESSIBILITY

Rock grain and bulk compressibility values (C_{grain} and C_b, respectively) are used to calculate specific storage (S_s), an important input parameter in WIPP PA calculations. Specific storage is defined as the fluid volume released from storage per unit decline in hydraulic head per unit bulk volume, and Equation 15 shows the relationship between specific storage and other rock parameters (Green and Wang, 1990).

$$S_s = \rho_f g \left[\left(\frac{1}{K_b} - \frac{1}{K_{grain}} \right) \left(1 - \frac{4G(1 - K_b/K_{grain})/3}{K_b + 4G/3} \right) + \phi \left(\frac{1}{K_f} - \frac{1}{K_{grain}} \right) \right] \tag{15}$$

where

ρ_f = fluid density

g = acceleration of gravity

K_b = drained bulk modulus of rock = $1 / C_b$

K_{grain} = unjacketed bulk modulus of rock (also known as grain, matrix or solids modulus) = $1 / C_{grain}$

G = drained shear modulus of rock

ϕ = porosity

K_f = bulk modulus of fluid.

Neither rock grain nor bulk compressibility has been measured for Salado halite or anhydrite material. Estimation of specific storage for PA calculations comes from two sources: (1) data in the literature for other halite and anhydrite samples (Beauheim, 1991) and (2) an $R^2 \times S_s$ term (where R is the effective wellbore radius) that results from interpretation of in situ borehole flow tests. Because the effective well-bore radius, R, is not a known parameter, inference of specific storage from in situ flow tests may not be justified. Grain and bulk compressibility should be independently measured for Salado rocks to support calculation of specific storage.

As so well stated by Scorer and Miller (1974), the term "rock compressibility" used without further qualification can be almost meaningless or at best incorrectly interpreted. Zimmerman et al. (1986), define four different rock compressibility relationships that relate changes in pore or bulk rock volume (V_p and V_b, respectively) to changes in pore or confining pressure (P_p and P_{conf}, respectively). As shown in Equations 16 and 17, two of these compressibility relationships are referred to as bulk compressibility, and the other two, shown in Equations 18 and 19, are referred to as pore compressibility.

Bulk Compressibility - Constant pore pressure, varying confining pressure:

$$C_{b,conf} = -\frac{1}{V_b}\left[\frac{\delta V_b}{\delta P_{conf}}\right]_{P_p} \tag{16}$$

Bulk Compressibility - Constant confining pressure, varying pore pressure:

$$C_{b,p} = \frac{1}{V_b}\left[\frac{\delta V_b}{\delta P_p}\right]_{P_{conf}} \tag{17}$$

Pore Compressibility - Constant pore pressure, varying confining pressure:

$$C_{p,conf} = -\frac{1}{V_p}\left[\frac{\delta V_p}{\delta P_{conf}}\right]_{P_p} \tag{18}$$

Pore Compressibility - Constant confining pressure, varying pore pressure:

$$C_{p,p} = \frac{1}{V_p}\left[\frac{\delta V_p}{\delta P_p}\right]_{P_{conf}} \quad . \tag{19}$$

In some cases, it may be useful to know or measure one or more of these compressibility relationships for a given rock sample. Because this may not always be practical, it is desirable to have some method of correlating the different compressibility values to each other. As derived by Zimmerman et al. (1986) for an idealized porous solid (i.e., isotropic, homogeneous, with elastic matrix containing void spaces of various shapes and sizes, which forms a completely connected network), the four rock compressibility relationships are not independent, and three

51

relationships can be found between them and porosity and rock grain compressibility. In the derivation of these relationships, applied pressures and the resulting strains are incremental changes superimposed on a pre-existing state of stress and strain. While the stress-strain relations that result from this analysis are nonlinear, representing the integration of incremental relations, the total strains will still be infinitesimal in the sense of classical linear elasticity. The boundary conditions assumed in the derivations are (1) uniform hydrostatic pressure, P_{conf}, over the entire outer surface of the porous body, and (2) uniform hydrostatic pressure, P_p, over the entire pore surface. Equations 20, 21, and 22 express the interrelationships among the rock compressibility relationships shown in Equations 16, 17, 18, and 19.

$$C_{b,p} = C_{b,conf} - C_{grain} \tag{20}$$

$$C_{p,conf} = (C_{b,conf} - C_{grain}) / \phi \tag{21}$$

$$C_{p,p} = [C_{b,conf} - (1+\phi) C_{grain}] / \phi \tag{22}$$

where

$$C_{grain} = \frac{1}{V_{grain}} \left[\frac{\delta V_{grain}}{\delta P_p} \right]_{P_{conf} - P_p} \tag{23}$$

C_{grain} = compressibility of the rock grain or matrix material = $1 / K_{grain}$

V_{grain} = volume of rock grain or matrix material.

The problem with this simplified approach is that most real rocks are neither isotropic, homogeneous, linear, elastic, nor have fully connected pores. Thus, these relationships may be in considerable error, and rock compressibility should be measured. An effort is under way to review methods for measuring rock compressibility and to develop an experimental-test matrix

for rock compressibility measurements. A detailed discussion of measurement system(s) for rock compressibility will be included in the Test Plan.

3.3.7.2 EFFECTIVE STRESS

For a given material property or process, the effective stress law is used to describe the appropriate stress state of a rock by defining a relationship between internal pore pressure, P_p, and confining stress, σ. A generalized effective stress law is shown in Equation 24, and the classical definition for net effective stress is shown in Equation 25 (Warpinski and Teufel, 1992). The classical definition for net effective stress is the effective stress law for $\alpha = 1.0$ so that the net effective stress is given by $\sigma - P_p$. While this definition, widely used in soil and hard rock analyses, assumes that α is constant, thereby resulting in a linear effective stress law, there is no reason that α cannot vary with either σ or P_p (Warpinski and Teufel, 1992).

$$P = G\,(\sigma - \alpha P_p) \qquad (24)$$

where

P	=	the specific material property or process (i.e., permeability, deformation, rock compressibility, or capillary pressure)
G	=	generalized function which describes the effect of stress on the property or process
σ	=	external confining stress on the sample (for hydrostatic conditions $\sigma = P_{conf}$)
P_p	=	pore pressure
α	=	poroelastic parameter that relates stress and pore pressure
$(\sigma - \alpha P_p)$	=	net effective stress.

$$\sigma' = \sigma - P_p \qquad (25)$$

where

σ'	=	net effective stress
σ	=	external confining stress on the sample (for hydrostatic conditions $\sigma = P_{conf}$)
P_p	=	pore pressure.

Warpinski and Teufel (1992) studied the effective stress law for permeability and deformation of tight sandstones and chalk and showed that the effective stress law is different for different processes. Their results for permeability measurements of tight sandstone, showed that α is near 1.0 for small stresses, but that behavior can become uncertain for large stresses. For the chalk samples, there was not a large amount of change in permeability with stress or pressure, so the effective stress law was of questionable value, although the effective stress behavior was very nonlinear. Sandstone deformation measurements resulted in α values ranging between 0.65 and 0.95, varying with both stress and pressure. For chalk deformation measurements, α was relatively constant: 0.8 in loading and 0.9 in unloading stress conditions. The researchers noted that agreement between their alpha values and those calculated from theoretical considerations was "poor," stating "the non-linear, anisotropic, nonhomogeneous behavior typical of rocks invalidates any theory of the effective stress law that is based on linear elasticity and constant material properties."

Warpinski and Teufel (1992) found low-permeability low-porosity rocks difficult to work with because many of the rock properties, including permeability and deformation, are dominated by microcracks that do not exist at in situ stress condition. They recommend that the effects of microcracks be eliminated or minimized to obtain acceptable measurements.

An effort is under way to more completely consider and evaluate the need for determining the effective stress laws for Salado single- and two-phase flow properties within the scope of this laboratory program. A detailed discussion of the need for effective stress law evaluation and (if necessary) test methodologies will be included in the Test Plan.

3.4 Program Milestones

Tentative milestones and a schedule for the Salado Two-Phase Flow Laboratory Program, which coincides with the roadmap exhibited in Figure 4, are shown in Figure 10. Program activities began in January 1992 with the initiation of scoping activities, and anhydrite experiments are scheduled to begin in FY94. The program life-span, including tests on halite material, is projected through FY97.

	FY92	FY93	FY94	FY95	FY96	FY97	FY98	FY99
Two-Phase Flow Program Test Plan	2/92 ▲	2/93 ▲ Prelim 9/93 ▲ Final						
Experiment Scoping Activities	2/92 ▲ 9/92 ▲							
Cooperative Program with GRS/KFA		3/93 ▲ - - -	- - ? (on hold)					
Preliminary Tests-Perm, Porosity Capillary Press and Core Damage	8/92 ▲		12/93 ▲					
Experiments			12/93 ▲ 6/94 ▲					
Reports			6/94 ▲ 9/94 ▲					
Develop Tool/ Techniques			3/94 ▲ 9/94 ▲					
Threshold/ Capillary Pressure		11/92 ▲ 6/93 ▲						
Relative Premeability		11/92 ▲ 6/93 ▲						
Set-Up Laboratory		2/93 ▲	9/94 ▲					
Single Phase (permeability-vs-porosity) —Report	11/92 ▲	1/93 4/93 6/93 ▲ D O B C	9/93 ▲ Tests	6/95 ▲ 6/95 ▲	12/95 ▲			
Two-Phase (relative perm, threshold press, capillary press) —Report		3/93 ▲ D	10/93 ▲ O 4/94 ▲ B 10/94 12/94 ▲ C Tests		6/96 ▲ 6/96 ▲	12/96 ▲		
Single Phase —Report			10/93 ▲ D, O,B	10/94 3/95 ▲ C Tests	6/96 ▲ 6/96 ▲	12/96 ▲		
Two Phase —Report				1/95 ▲ D, B,O	12/95 4/96 ▲ C Tests	4/97 ▲ 4/97 ▲ 9/97 ▲		

D = Design/Develop
O = Order
B = Build
C = Calibrate

Core Damage / Assess Methods / Anhydrite Tests / Halite Tests / Tests

TRI-6119-124-0

Figure 10. Salado Two-Phase Flow Laboratory Program tentative schedule and milestones.

FY92 was spent defining the program in terms of identifying the customers and their needs, determining which Salado or other materials to test, test priorities, which state-of-the-art technologies are available and applicable for the tests, and identifying potential showstoppers/outstanding issues that must be addressed. Table 2 summarizes those activities, including a listing of the issues, how they were addressed, and the resolution.

The tasks outlined for FY93 fall into three categories: Scoping Activities, Program Development Activities, and Experimental Scoping Activities. Table 3 summarizes FY93 scoping activities, which consist of (1) the evaluation of two-phase flow technologies for measurement of threshold and capillary pressure and relative permeability and (2) preliminary scoping experiments. Program Development activities, exhibited in Table 4, include the completion of a program test plan, the establishment of a collaborative program with German scientists at GRS/KFA, and the development of rock and single- and two-phase flow laboratory facilities at SNL. Table 5 summarizes the experimental activities, including core characterization, core damage assessment, and rock and flow properties. Table 5 also identifies the properties that will be measured and the type and number of tests that will be performed in FY93.

FY94 will be spent performing single-phase flow experiments, designing and building two-phase flow equipment, and initiating the threshold pressure and relative permeability tests for anhydrite. Laboratory tests and reporting will continue through FY97.

Table 2. Summary of FY92 Scoping Activities

Issue	How Addressed	Outcome
Who are the Customers?	Meetings and Discussions with Fluid Flow and Transport and PA	Customers were Identified. 1. WIPP Numerical Modelers (PA) 2. WIPP Fluid Flow Analysts (AITU) 3. WIPP Fluid Flow Modelers (AITU)
What Rock and Flow Properties Should be Measured?	1. Discussions with AITU Analysts and Modelers 2. Discussions with PA 3. Sensitivity Analyses 4. Technology Advisory Group	Rock and Flow Properties were Identified. 1. Porosity (Total and Interconnected) 2. Permeability vs Stress 3. Rock Compressibility 4. Capillary and Threshold Pressure 5. Relative Permeability 6. Standard Petrographic Analysis
What Stratigraphic Units/Materials Should be Tested and in What Order of Priority?	1. Discussions with AITU Analysts and Modelers 2. Discussions with PA	Stratigraphic Units and Materials were Identified (In Order of Priority). 1. Anhydrite Interbeds 2. Halite 3. Impure Halite 4. Backfill Material 5. Seal Material
What are the State-of-the-Art Technologies Available for the Measurement of these Rock and Flow Properties?	1. Technical Discussions with Expert Core Analysts and Visits to Rock and Flow Laboratories: SNL Core Lab, TerraTek, RE SPEC, NM Tech, CNM, CoreLab, USGS and IUT 2. Literature Search and Review	Reports Investigations of Laboratory Techniques to Measure are in Progress. 1. Relative Permeability 2. Capillary and Threshold Pressure
Are There Any Outstanding Issues?	1. Discussions with AITU Analysts and Modelers 2. Discussions with PA 3. Technical Discussions with Expert Core Analysts and Visits to Rock and Flow Laboratories: SNL Core Laboratory, TerraTek, RE SPEC, NM Tech, CNM, CoreLab, USGS and IUT 4. Technology Advisory Group	Outstanding Issues Were Identified. 1. Damage to Sample During Coring and Preparation* 2. Technology Limitations for Two-Phase Flow Measurements* 3. Time Constraints 4. Budget Constraints * Focus of FY93 Experimental Scoping Activities

Table 3. Summary of FY93 Scoping Activities

Activity	Status
Determine appropriate tests for each two-phase flow parameter	Review of technical literature on two-phase flow underway
Perform preliminary experiments to identify potential problems	Preliminary scoping experiments underway (See Table 4)

Table 4. Summary of FY93 Program Development Activities

Activity	Status
Establish Collaborative Program with GRS/KFA in Germany	Collaborative program development meetings held in Julich, Germany in November 1992 German program is unfunded German program will focus on halite; no interest in salt/shale at this time Collaborative efforts on hold Will reevaluate collaborative program in December 1993
Establish Two-Phase Flow Laboratory Facility at SNL	Arrangements made to use SNL K117 testing equipment Contract submitted for design of single- and two-phase flow experimental apparatus (est. placement by 4/94) Contract submitted for pulse decay permeameter and permeameter test (delivery 6/94) Efforts underway to find space at SNL for laboratory Core QA procedure development underway
Complete Salado Two-Phase Flow Laboratory Program Test Plan	Conceptual Plan completed (this document) Test Plan to be completed in September 1994

Table 5. Summary of FY93 Experimental Scoping Activities*

Property	Test	Number of Tests
Core Sample Characterization		
Standard petrographic examination and X ray diffraction	X ray Diffraction	12
	Light Microscopy	12
Core Damage Assessment		
Function of Coring Rate [?]	Epoxy impregnation	2
Coring Induced Damage [?]	CT Scan Imaging - Whole Core	1 (4 ft x 6 in core)
Sample Preparation Induced Damage [?]	CT Scan Imaging - Sub Cores with liquid flowing through core during scan	3 (4 in x 4.5 in core)
Rock and Flow		
Porosity	Total	7
	Interconnected	40
Single Phase Permeability	Gas - Parallel to bedding plane (horizontal)	22
	Gas - Perpendicular to bedding plane (vertical)	10
	Brine - Parallel to bedding plane (horizontal)	6
	Non reactive liquid - Mineral Spirits (horizontal)	6
Capillary Pressure	Mercury Injection	10
	Centrifuge	10

* All tests to be performed on Marker Bed 139 anhydrite core samples

4.0 SITE SUPPORT

Because the two-phase flow tests will take place at SNL's Albuquerque location or at a contractor's laboratory facility, limited WIPP-site support will be required. The core material necessary for these tests will require drill-coring and core-logging services provided by the WIPP Management and Operating Contractor (MOC). These and any additional services will be coordinated through the SNL manager of WIPP-site operations, using standard procedures.

Anticipated services will be identified at the completion of preliminary tests and will be addressed in the Test Plan.

5.0 OPERATIONS

5.1 Personnel Responsibilities (Delegation of Authority)

The following procedures and program policies apply to test implementation and operation.

5.1.1 Site Operations Test Activities

The WIPP Site Operations Department (6343) Manager is responsible for coordinating site activities and ensuring worker safety at the WIPP site. As part of these overall site duties, the manager is specifically responsible for:

- coordinating SNL requirements with DOE and the Westinghouse Electric Corporation's Waste Isolation Division (WID);

- coordinating overall test operations between SNL and WID Experimental Operations;

- controlling and coordinating all underground visits to the test areas;

- reporting progress of the test activities to SNL management, DOE, and WID as deemed appropriate;

- managing the safety and security requirements for SNL underground testing programs.

5.1.2 Technical Direction

S.M. Howarth (Department 6119, phone (505) 844-0303) is the Principal Investigator (PI) for the technical work to be performed under this conceptual plan. Howarth has primary

responsibility for the two-phase flow laboratory program. The PI has responsibility for conducting the tests within the following specific areas of authority:

- test objectives and test configurations;

- direction of WIPP-site and laboratory contractors;

- selection of locations for coring, and selection and approval of equipment design and modifications;

- determination of experiment operating parameters, such as pressures, rates of pressure buildup, flow rates, test fluids, test duration, data acquisition sampling rates, and other parameters related to the conduct of tests;

- test analysis;

- approval of any proposed changes to the testing equipment and procedures;

- approval of procedures for documentation and control of field and laboratory log books;

- approval of installation forms, calibration forms, data readings, etc.;

- preparation of data reports, analyses, and evaluations;

- approval for data dissemination and report distribution, both within SNL and externally.

5.1.3 WIPP Quality Assurance Chief

S.Y. Pickering (Department 6303, phone (505) 887-8430; WIPP site) is the WIPP Quality Assurance (QA) Chief with the following responsibilities:

- to establish and maintain a documented and approved "Quality Assurance Program Description (QAPD)";

- to conduct periodic QA audits to ensure compliance with the QAPD;

- to ensure that data are acquired and maintained in accordance with QA requirements;

- to review and approve test and reporting procedures to verify that all experimental work is conducted in accordance with those procedures;

- to ensure that staff are appropriately trained and operationally familiar with QA requirements;

- to review Nonconformance Reports and verify implementation of corrective actions;

- to ensure that all gages and instruments are calibrated in accordance with documented calibration procedures, using standards that are traceable to nationally recognized standards;

- to ensure that SNL QA requirements are transmitted to contractors associated with the testing program; and

- to coordinate Sandia QA and Westinghouse QA personnel.

5.2 Test Schedule

Nonexperimental scoping activities associated with this conceptual plan began in January 1992. Experimental scoping activities began in October 1992 and will continue through calendar year 1993. The results and recommendations from these scoping activities will be used to establish the scope of the Test Plan for the Two-Phase Flow Laboratory Program.

5.3 Operational Safety and Environment

5.3.1 Safety Requirements

The equipment for this testing program will consist of commercially acquired or SNL-fabricated components that will be rated for appropriate maximum allowable operating pressures. Pressure ratings of individual parts, such as valves and pressure lines, are either marked by the supplier or documented in data packages according to guidelines of the SNL Department 6343 Safety Representative for WIPP Site Operations or the SNL 6100 or 6300 Pressure Safety Advisor for WIPP site test operations or SNL New Mexico laboratory operations, respectively.

Operational safety will be addressed through the SNL Environmental Safety and Health (ES&H) standard operating procedures (SOPs) developed by the site supervisor, and other relevant procedures. Project-specific WIPP-site safety procedures will be approved through the PI, WIPP-site safety personnel, and the SNL safety organization. The ES&H SOP's include:

- identification of potential hazards;
- emergency shutdown procedures;
- personnel to be contacted in case of emergencies.

5.3.2 Environment

SNL facility and WIPP-site environmental considerations of the specific Two-Phase Flow Laboratory Program tests will be determined once the appropriate testing techniques and methods are identified. Environmental concerns will be addressed in the Two-Phase Flow Laboratory Program Test Plan.

6.0 SPECIAL TRAINING

Personnel responsible for performing the tests within the Two-Phase Flow Laboratory Program will be trained in the design and operation of the test equipment and in all attendant safety procedures. A formal safety briefing will be part of the testing procedures and all personnel will affirm that they have read and understood the relevant SOPs for the laboratory and WIPP-site tests. No additional special training is anticipated.

7.0 TEST MANAGEMENT

7.1 Test Plan Review and Approval

The "Test Plan: Two-Phase Flow Laboratory Program For The Waste Isolation Pilot Plant" will be reviewed and approved according to standard SNL/WIPP procedures. This conceptual plan will be reviewed according to all applicable SNL guidelines for SAND reports.

7.2 Management Interface

Development of the WIPP is the responsibility of the DOE and is supported by two major participants: SNL and Westinghouse Electric Corporation. The Technology Development Program is the responsibility of Sandia. Westinghouse Electric Corporation's WID is the MOC for the WIPP facility, which includes design support, overall safety assurance support, facility operations, and environment and institutional support.

The drill-coring and core-logging required to support the tests described in this document will be implemented by SNL with the assistance of WID experimental support personnel under the direction of SNL. Coordination of coring activities may include the procurement of needed hardware, implementation of coring activities, and preparation of interface documents.

In accordance with the management organization, the SNL PI is responsible for all aspects of the tests, from planning to final data analysis and evaluation of the results. The PI reports to the Fluid Flow and Transport Department (6119) of the Geoscience and Geotechnology Center (6100). The PI will also direct, as needed, the activities of other organizations and contractors through the matrix management structure established within SNL.

7.3 Procurement Procedures

Services, material, and equipment for the testing program will be procured by the SNL Purchasing Organization (7216) or through SNL's contractors, using DOE-accepted procedures and practices. Purchases of hazardous materials must be approved the SNL Safety Representative for WIPP Site Operations if the materials are intended to be used at the WIPP. Procured materials and equipment will be shipped to SNL Shipping and Receiving Division (3912) and transferred to an assembly point at SNL or to the designated SNL or subcontractor representative at the WIPP site. Items can be shipped directly to the WIPP site and will be properly received by the designated SNL or subcontractor representative at the site.

7.4 Quality Assurance Requirements

All SNL tests are implemented in accordance with SNL's Waste Isolation Pilot Plant "Quality Assurance Program Description (QAPD)." The QAPD meets the requirements of NQA-1-1989, DOE 5700.6c, and Chapter 11 of the *Final Safety Analysis Report*. This QA plan has been approved by the DOE/WPIO and DOE/WPSO for all WIPP activities assigned to SNL and is specific to the WIPP Project. Contractor personnel working with SNL personnel, either at the WIPP site or in Albuquerque, are subject to the WIPP QAPD or their own SNL-approved QA program. Specific applications of the WIPP QAPD to the present tests have been incorporated throughout this conceptual plan.

Documentation of the preparation for this experiment may include:

- the test plan and appropriate approvals;

- photographs showing equipment and interconnections of apparatus;

- instrument calibration records;

- notebooks, logbooks, WIPP procedures, worksheets, and forms for installation and operation.

The PI, contractors, or personnel designated by the PI will be responsible for data acquisition and storage and for assuring that all documentation at the WIPP site is maintained in accordance with the WIPP QAPD. Deviations from test plans and nonconformances or unusual occurrences will also be recorded in Test Plan Appendices, and appropriate forms will be completed.

7.5 Data Transfer

Throughout the tests, data will be acquired and documented in notebooks and on floppy disks. Copies of all basic data reports and interpretive reports with accompanying analyses/evaluations will be transferred through DOE/WPIO to interested agencies, institutions, and scientific and engineering communities for application to radioactive waste projects. Photographs for technical examination, illustrations, and records will be made available for technical evaluation as well as for public viewing, as authorized by the DOE/WPIO.

8.0 REFERENCES

Amyx, J.W., D.M. Bass, Jr., and R.L. Whiting. 1960. *Petroleum Reservoir Engineering: Physical Properties*. New York, NY: McGraw-Hill, Inc.

API (American Petroleum Institute). 1956. *Recommended Practice for Determining Permeability of Porous Media*. API RP 27. Washington, DC: American Petroleum Institute.

API (American Petroleum Institute). 1960. *Recommended Practice for Rock Core-Analysis Procedure*. API RP 40. Washington, DC: American Petroleum Institute.

Basan, P., J.R. Hook, K. Hughes, J. Rathmell, and D.C. Thomas. 1988. "Measuring Porosity, Saturation and Permeability from Cores: An Appreciation of the Difficulties," *The Technical Review (A Schlumberger Publication)*. Volume 36, no. 4, 22-36.

Bass, D.M., Jr. 1987. "Properties of Reservoir Rocks," *Petroleum Engineering Handbook*. Ed. H.B. Bradley. Richardson, TX: Society of Petroleum Engineers. Chapter 26.

Beauheim, R.L., G.J. Saulnier, Jr., and J.D. Avis. 1991. *Interpretation of Brine-Permeability Tests of the Salado Formation at the Waste Isolation Pilot Plant Site: First Interim Report*. SAND90-0083. Albuquerque, NM: Sandia National Laboratories.

Black, S.R., R.S. Newton, and D.K. Shukla, eds. 1983. *Results of the Site Validation Experiments. Volume II, Supporting Document 14*. TME 3177, Rev. 2.0. Carlsbad, NM: US Department of Energy.

Brace, W.F., J.B. Walsh, and W.T. Frangos. 1968. "Permeability of Granite Under High Pressure," *Journal of Geophysical Research*. Vol. 73, no. 6, 2225-2236.

Brooks, R.H., and A.T. Corey. 1964. *Hydraulic Properties of Porous Media*. Hydrology Paper No. 3. Fort Collins, CO: Colorado State University.

Davies, P.B. 1989. "Preliminary Threshold Pressure Estimates and Status of Two-Phase Simulation of Waste-Generated Gas," *National Academy of Sciences WIPP Review Panel, Half Moon Bay, CA, December 13, 1989*. (Copy on file at the Waste Management and Transportation Library, Sandia National Laboratories, Albuquerque, NM).

Davies, P.B. 1991. *Evaluation of the Role of Threshold Pressure in Controlling Flow of Waste-Generated Gas into Bedded Salt at the Waste Isolation Pilot Plant*. SAND90-3246. Albuquerque, NM: Sandia National Laboratories.

Davies, P.B., G. Freeze, M. Reeves, and T. Cauffman. 1990. "Status Report on Multi-Phase Simulations of Waste-Generated Gas at the WIPP Repository," *National Academy of Sciences WIPP Review Panel, Washington, DC, September 19, 1990.* (Copy on file at the Waste Management and Transportation Library, Sandia National Laboratories, Albuquerque, NM).

Davies, P.B., L.H. Brush, M.A. Molecke, F.T. Mendenhall, and S.W. Webb, eds. 1991. *Waste-Generated Gas at the Waste Isolation Pilot Plant: Papers Presented at the Nuclear Energy Agency Workshop on Gas Generation and Release from Radioactive Waste Repositories.* SAND91-2378. Albuquerque, NM: Sandia National Laboratories.

Davies, P.B., R.L. Beauheim, and E.D. Gorham. 1992. Appendix A: "Additional Comments on Far-Field Anhydrite Permeability Distribution in 'PA Modeling Using BRAGFLO—1992' 7-8-92 Memo by J. Schreiber," *Preliminary Performance Assessment for the Waste Isolation Pilot Plant, December 1992. Volume 3: Model Parameters.* Sandia WIPP Project. SAND92-0700/3. Albuquerque, NM: Sandia National Laboratories. A-39 through A-45.

Fatt, I., and D.H. Davis. 1952. "Reduction in Permeability with Overburden Pressure," *Petroleum Transactions, AIME.* Vol. 195, 329.

Freeman, D.L., and D.C. Bush. 1983. "Low-Permeability Laboratory Measurements by Nonsteady-State and Conventional Methods," *Society of Petroleum Engineers Journal.* Vol. 23, no. 6, 928-936.

Gorham, E. 1993. "Appendix A: Documentation of RCRA Recommendations to PA for Salado Formation Permeability and Pore Pressure," *Conceptual Plan: Two-Phase Flow Laboratory Program for the Waste Isolation Pilot Plant.* S.M. Howarth. SAND93-1197. Albuquerque, NM: Sandia National Laboratories.

Gray, D.H., I. Fatt, and G. Bergamini. 1963. "The Effect of Stress on Permeability of Sandstone Cores," *Society of Petroleum Engineers Journal.* Vol. 3, no. 2, 95-100.

Green, D.H., and H.F. Wang. 1990. "Specific Storage as a Poroelastic Coefficient," *Water Resources Research.* Vol. 26, no. 7, 1631-1637.

Hsieh, P.A., J.V. Tracy, C.E. Neuzil, J.D. Bredehoeft, and S.E. Silliman. 1981. "A Transient Laboratory Method for Determining the Hydraulic Properties of 'Tight' Rocks -- 1. Theory," *International Journal of Rock Mechanics and Mining Sciences & Geomechanics Abstracts.* Vol. 18, no. 3, 245-252.

Jones, F.O., and W.W. Owens. 1980. "A Laboratory Study of Low-Permeability Gas Sands," *Journal of Petroleum Technology.* Vol. 32, no. 9, 1631-1640.

Keelan, D.K. 1972. "A Critical Review of Core Analysis Techniques," *The Journal of Canadian Petroleum Technology*. Vol. 11, no. 2, 42-55.

Klinkenberg, L.J. 1941. "The Permeability of Porous Media to Liquids and Gases," *API Drilling and Production Practice*. 200-213.

McLatchie, A.S., R.A. Hemstock, and J.W. Young. 1958. "The Effective Compressibility of Reservoir Rock and Its Effects on Permeability," *Journal of Petroleum Technology*. June 1958, 49-51.

Morrow, N.R., J.S. Ward, and K.R. Brower. 1986. *Rock Matrix and Fracture Analysis of Flow in Western Tight Gas Sands - 1985 Annual Report*. DOE/MC/21179-2032. Socorro, NM: New Mexico Institute of Mining and Technology, New Mexico Petroleum Recovery Research Center.

Parker, J.C., R.J. Lenhard, and T. Kuppusamy. 1987. "A Parametric Model for Constitutive Properties Governing Multiphase Flow in Porous Media," *Water Resources Research*. Vol. 23, no. 4, 618-624.

Rechard, R.P., H. Iuzzolino, and J.S. Sandha. 1990. *Data Used in Preliminary Performance Assessment of the Waste Isolation Pilot Plant (1990)*. SAND89-2408. Albuquerque, NM: Sandia National Laboratories.

Rose, W. 1987. "Relative Permeability," *Petroleum Engineering Handbook*. Ed. H.B. Bradley. Richardson, TX: Society of Petroleum Engineers. Chapter 28.

Rudd, N. 1974. "New Techniques for Threshold Pressure Determination in Gas Storage Cap Rock " *Geo-Engineering Laboratories, Inc. Tech Memo No. 6*. Chicago, IL: Institute of Gas Technology.

Saulnier, G.J., Jr. 1992. "Test Plan: Gas-Threshold-Pressure Testing of the Salado Formation in the WIPP Underground Facility." Albuquerque, NM: Sandia National Laboratories. (Copy on file at the Waste Management and Transportation Library, Sandia National Laboratories, Albuquerque, NM).

Scorer, J.D.T., and F.G. Miller. 1974. *A Review of Reservoir Rock Compressibility, and Its Relationship to Oil and Gas Recovery*. IP-74-003. London, England: Institute of Petroleum.

Thomas, L.K., D.L. Katz, and M.R. Tek. 1968. "Threshold Pressure Phenomena in Porous Media," *Society of Petroleum Engineers Journal*. Vol. 8, no. 2, 174-184.

Warpinski, N.R., and L.W. Teufel. 1992. "Determination of the Effective Stress Law for Permeability and Deformation in Low-Permeability Rocks," *SPE Formation Evaluation*. Vol. 7, no. 2, 123-131.

Webb, S.W. 1992. "Appendix A: Two-Phase Characteristic Curves," *Steady-State Saturation Profiles for Linear Immiscible Fluid Displacement in Porous Media*. S.W. Webb. SAND91-2924. Albuquerque, NM: Sandia National Laboratories. A-1 through A-6.

Zimmerman, R.W., W.H. Somerton, and M.S. King. 1986. "Compressibility of Porous Rocks," *Journal of Geophysical Research*. Vol. 91, no. B12, 12,765-12,777.

9.0 ACRONYM LIST

API	American Petroleum Institute
API RP	American Petroleum Institute Recommended Practice
CSM	Colorado School of Mines; Golden, Colorado
CT	Computed Tomography or Computer Aided Tomography
DOE	U.S. Department of Energy
IGT	Institute for Gas Technology; Chicago, Illinois
LM	Light Microscopy
MB 139	Marker Bed 139
MOC	Management and Operating Contractor
NAGRA	Switzerland's national consortium for safe nuclear waste disposal
NAS	National Academy of Sciences
NMR	Nuclear Magnetic Resonance imaging
PA	Performance Assessment
PI	Principal Investigator
QA	Quality Assurance
QAPD	Quality Assurance Program Description
RE/SPEC	RE/SPEC Inc.; Rapid City, South Dakota
RCRA	Resource, Conservation, and Recovery Act of 1976 (Public Law 94-580) and subsequent amendments (e.g., HSWA - Hazardous and Solid Waste Amendments of 1984)
SCA	Society of Core Analysts

SEM	Scanning Electron Microscope
SNL	Sandia National Laboratories
SOP	Standard Operating Procedure
SPE	Society of Petroleum Engineers
TAG	Technical Advisory Group
USGS	U.S. Geological Survey
WID	Waste Isolation Division of Westinghouse Electric Corporation
WIPP	Waste Isolation Pilot Plant
WPIO	WIPP Project Integration Office
WPSO	WIPP Project Site Office
XRD	X-ray Diffraction

APPENDIX A

Gorham, E.D. 1992. "Documentation of RCRA Recommendations to PA for Salado Formation Permeability and Pore Pressure." Internal memorandum to B. Butcher, 6342. Albuquerque, NM: Sandia National Laboratories. August 19, 1992.

date: August 19, 1992

to: Barry Butcher, 6342

from: Elaine Gorham, 6119, 4-1401

subject: Documentation of RCRA Recommendations to PA for Salado Formation Permeability and Pore Pressure

Attached is complete documentation of the rationale for the 6119 recommendation to PA for the RCRA calculations. In this document we remained true to our original recommendations, although, now that we understand your models better, we would change the recommendations.

You may publish the documentation as part of your RCRA documentation. The format we used is more appropriate for publication than memos.

If this format seems appropriate for your purposes we will record our 40 CFR 191 Part B recommendations in a similar format shortly. If you have any questions or comments, please call me.

Distribution

6100	P. Hommert, Acting
6119	R. Beauheim
6119	P. Davies
6119	S. Howarth
6119	S. Webb
6300	D. Miller
6303	W. Weart
6342	D. R. Anderson
6342	M. Tierney
WPIO	R. Becker

Recommendations to PA on
Salado Formation Intrinsic Permeability and Pore Pressure
for
RCRA Calculations

April 1, 1992

Elaine Gorham
Richard Beauheim
Peter Davies
Susan Howarth
Stephen Webb

Department 6119

Introduction

In March 1992, the Fluid Flow and Transport Department was asked to recommend Salado Formation permeability and pore pressure probability distributions to be used in the 1992 RCRA calculations for the WIPP. The recommendations were requested and transmitted informally. This description is to satisfy the requirement to record the recommendations supplied on April 1, 1992 and the rationale for them.

Since input parameters, such as permeability or formation pore pressure, are, for the most part, inferred from complex hydrologic tests, the interpretive model assumptions should be compatible with the predictive or performance assessment model in which the parameters will be used. Thus a suggested excavation geometry and zoning scheme was supplied along with recommended distributions for permeability and pore pressure. The recommended initial geometry is shown in Figure 1 and the distributions suggested for permeability and pore pressure (Table 1 and Figures 2-8) were referenced with respect to those zones.

Our Assumptions

Assumptions about the models to be used in the PA calculations that were essential in formulating the RCRA data recommendations were not included in any written material transmitted to the Performance Assessment Department. Our assumptions were

1. The Salado Formation was described as consisting of layers of either halite or anhydrite. Parts of the Salado Formation described as argillaceous halite were lumped with the halite; clay seams were lumped with the type of lithology in which they occurred. Anhydrites a and b were lumped together.

2. The Salado Formation was isotropic and homogeneous within each layer of halite or anhydrite. The halite and anhydrite have interconnected porosity.

3. The repository will have been open, dry and at atmospheric pressure for at least 30 years before the performance assessment calculations begin, that is, during the repository operational phase. An explicit calculation of formation depressurization or other effects resulting from the operational phase will not be performed as part of the PA calculations but will be taken into account in the initial conditions of the calculation.

4. Excavation closure effects will be included in the PA model **as well as pressurized fracture opening in the anhydrite beds.** [These assumptions were incorrect, as it was later learned that neither of these processes were modeled in the PA RCRA calculations.] Pressurized fracture opening in the anhydrite beds may have the potential to significantly increase far-field interbed permeabilities.

5. The nature of the disturbed rock zone (DRZ) is uncertain, reflecting the diversity of technical hypotheses that have been formulated, documented and undocumented. These include the hypothesis that the DRZ is a zone of increased porosity surrounding the excavation, that is stable in extent or increasing in extent with the age of the excavation. Other hypotheses concerning the nature of the DRZ are that the bulk properties of the halite within the DRZ are unchanged, but that within the DRZ fractures form that result in a large increase in permeability with a relatively small increase in porosity or storativity within the DRZ. The size of the DRZ c r vary from a few inches into the formation from an excavation surface to a few "room-radii" away from the excavation surface. It was assumed that all possible descriptions of the DRZ should be included in the probability distributions for permeability and porosity in the DRZ.

6. The DRZ does not reconsolidate during the post-closure calculations due to repository re-pressurization or creep closure of the excavation.

Sources of uncertainty in interpreting data.

The process of inferring permeability from a hydrologic pulse or shut-in test requires that one make an assumption about the diffusivity or specific storage in the formation, about the size of a damaged zone surrounding the test zone, and that the compressibility of the test-zone fluid is constant and can be quantified by a single measurement of fluid withdrawn from the test zone vs test zone pressure drop during withdrawal. A value of specific storage calculated using literature values for halite and and brine compressibilities may not be correct. Recent improvements in the measurement of permeability involve combining a constant-pressure flow test and a shut-in test to directly infer a value of specific storage. However, the improved interpretive technique was used only on permeability tests SCP01, S1P73-B, C1X10, L4P52-A and L4P51-B. For the remaining permeability tests, what is in reality obtained is a value of permeability **given an**

assumed value of specific storage. Sensitivity calculations have shown that our inferred permeability values may range over one order of magnitude as our assumed values of specific storage range over three orders of magnitude. (Beauheim et al, 1990; Beauheim et al, 1992) Inasmuch as our assumed values of specific storage do not range over more than three orders of magnitude, we estimate our uncertainty in permeability to be about an order of magnitude.

Other assumptions in analysis of permeability tests include the assumption that gas dissolved in formation brine does not significantly affect the permeability interpretation and that significant amounts of free gas are not present in the formation. In numerous permeability tests, gas was observed to bubble from the formation shortly after the test zone was drilled. A sensitivity analysis is planned for FY93 in which the effect of these phenomena on permeability interpretation will be investigated. For the RCRA recommendations, Rick Beauheim, who has been conducting interpretations of permeability tests, provided the (subjective) input that resulted in an order of magnitude confidence in interpreted permeability values.

Uncertainties in the interpretation of brine-inflow tests are due to (a) scatter in the brine-inflow data and (b) the use of a one-dimensional model which neglects loss of fluid to the surface of the excavation and assumes a uniform pore pressure unaffected by the excavation. In a one-dimensional data analysis by McTigue (1992), it was found that the uncertainties in the inferred values of diffusivity due to data scatter could be substantial. Uncertainties in inferred values of permeability may be smaller. (See Table 2.) In addition, recent analyses (Gelbard, 1992) indicate that the use of a one-dimensional model may introduce significant errors in the interpretation of diffusivity and permeability from brine-inflow data.

Rationale for Formulating Permeability Distributions

Table 3 represents a current (as of 1/5/92) compilation of interpreted values of permeability and formation pressure from the Permeability Testing Program, the Small-Scale Brine Inflow Program and Room Q. For the 1992 RCRA PA calculations, interpreted values of permeability in Table 3 were classified according to the regional map shown in Figure 1.

The disturbed rock zone is poorly defined. For these recommendations, test zones were classified as being in the disturbed rock zone if the zone could sustain little or no formation pressure and if the permeability of the zone was clearly higher than expected in competent rock.

The tests for which a reasonable pressure could be sustained in the test zone, but the pressure was not high enough to approach our (subjective) estimate of the far field pressure, were classified as being in a "depressurized" zone. The "depressurized zone" is

hypothesized as having experienced some hydraulic depressurization and possibly some elastic stress relief due to the excavation, but probably no irreversible rock damage and large permeability changes. Clearly, the depressurized zone extent will be different in higher permeability layers, such as the Marker Beds, than in lower permeability layers, such as pure halite. It is important to note that the depressurized zone is not a disturbed rock zone; the data from the depressurized zones do not support the hypothesis that the permeability, and the interconnected porosity, are greatly different in the depressurized zones from their far field values.

The latter classifications of test zones are subjective and will be examined in more detail as the Fluid Flow and Transport Department improves interpretation techniques and understanding of the rock matrix.

For the tests in Table 3, other than the Room Q tests, the disturbed rock zone, if in fact it has a clear boundary and if it has a significant extent, was hypothesized to extend about one meter from the excavation into the formation. The boundary of the depressurized zone in the Marker Beds was hypothesized to be approximately 10 meters from the excavation. These hypotheses formed the basis for the geometrical treatment of the excavation suggested in Figure 1. Detailed repository depressurization calculations are planned for FY93.

The probability distributions recommended for the PA calculations were formulated so as to reflect the true range of scientific uncertainty in the parameter values supplied, including uncertainty due to measurement error and uncertainty due to interpretation ambiguities. As mentioned above, an order of magnitude uncertainty in the interpreted value of permeability was used as a rule of thumb for creating recommended probability distributions.

All measurements of permeability were given equal weight, except those values derived from brine inflow measurements in 36" diameter holes in Room D. Those tests were considered flawed and deleted from the list because of the uncertain history of the excavation surrounding the test zone (Finley, 1992).

The hypothesis that permeabilities in the Salado Formation are heterogeneous is given much weight in the Fluid Flow and Transport Department. The use of a single uniform value for all halite and argillaceous halite regions, and a different uniform value for all marker beds implies that the permeability values used in the PA calculations should be "effective" values that are rigorously derived from our measurements. A systematic approach for defining such an "effective" value has not yet been outlined, but will be investigated in FY93. This aspect of formulating the distribution was ignored for these recommendations.

Given the assumptions and difficulties outlined above, differential probability distributions were formed by marking the locations

along a permeability axis of the results of the tests in Table 3. The number of tests in each $\log_{10}$ interval were used to indicate the relative probability that the true value lay in that interval. Cumulative probability distributions listed in Table 1 can be formulated from the differential probability distributions in Figures 2-8. Test results that were "Too low to measure" were assigned an equal probability of lying between a true 0 value and 1.0×10^{-24} m^2. Thus, the abscissa of Figure 2 is logarithmic between 10^{-24} and 10^{-21} and linear between 0 and 10^{-24}.

Rationale for Formulating Pore Pressure Distributions

The measurement of test-zone pore pressure is straightforward and is only accomplished in the Permeability Testing Program and the Room Q permeability tests. If, during a pressure build-up test or pulse-withdrawal test, the pressure reaches a steady state pressure, that pressure is interpreted as the formation pore pressure at the location of the test zone. If a steady-state pressure is not reached before the test is terminated, some technique must be used to extrapolate the formation pore pressure from the shape of the pressure-vs-time curve.

For the tests listed in Table 3, all pressures listed are measured or estimated values of formation pore pressure. The far field formation pore pressures measured in the anhydrite layers yield a fairly consistent measurement of 12.5+-0.1 MPa. It is not understood why the pore pressure measured in the single halite far field test is significantly lower than those reached in the anhydrite far field. Possibilities include: (a) The regions in the halite that have non-zero permeability are not interconnected with higher pressure regions such as the anhydrite layers; (b) the regions in the halite that have non-zero permeability have not reached pressure equilibrium with the anhydrite layers; or (c) pore dilation (and accompanying depressurization) in response to excavation and/or drilling affects halite to a greater distance than anhydrite.

Based on current measurements, it cannot be ruled out that substantial regions of the Salado Formation will be at significantly lower initial pore pressure than the anhydrite layers. Thus it was recommended that the performance assessment calculations include this possibility in the RCRA calculations.

Since the effect of excavation on the formation is still poorly understood, from a hydrological viewpoint, it is uncertain that tests believed to be in the far field are indeed in the far field. It was recommended that the halite pore pressure reflect the single value measured, 9.5 MPa, with an uncertainty of 0.5 MPa and the anhydrite pore pressure reflect the average value measured, 12.5 MPa, also with an uncertainty of 0.5 MPa. It is recognized that this recommendation is not consistent with the equilibrium, continuum assumptions implicit in the PA and the 6119 repository scale modeling. (The assumption of formation hydraulic equilibrium

can be tested using existing models and assumed values of halite
and anhydrite permeability. Such a calculation may be performed by
Department 6119 in the future.)

In order to reproduce some of the effects of depressurization of
the Salado Formation that would have occurred during the disposal
phase of the repository, several additional recommendations were
made concerning the initial conditions for the PA calculations:
All disturbed zones, except for MB 138, should be fully saturated
but at zero initial pore pressure. Because of its distance from
the excavation MB 138 could remain slightly pressurized at the
start of the disposal phase. Thus pore pressures in MB 138 should
be sampled from an even probability distribution from 0 to 4 MPa.
In the "depressurized regions" of both halite and anhydrite the
pressures should vary smoothly between the values of the
surrounding formations. For example, the pressure below MB 139
should rise smoothly from 0 in the disturbed zone to the value
assumed for the far field at distances of 11 or more meters from MB
139. Specific recommendations for initial pore pressures are
included in Table 3 for each of the zones described in Figure 1.

**Afterthoughts and Comments on the Effect of Data Recommendations on
RCRA Calculations.**

Communications with the PA Department subsequent to making the
recommendations outlined above have revealed that some of the
assumptions outlined above concerning the PA model were not
correct. An important aspect of the current PA model for the
Salado Formation is its inability to simulate pressure-induced
fracturing in the anhydrite layers, a phenomenon that has been
experimentally demonstrated at the WIPP. The phenomenon may
enhance the migration of gas into the formation as the gas pressure
in the repository builds up. Thus it is possible that the current
PA model underpredicts lateral gas migration.

Finally, the recommendations of the Fluid Flow and Transport
Department were not fully implemented in the RCRA compliance
calculations, because of insufficient time to eliminate the
inconsistencies between the PA modeling approach and the Department
6119 recommendations.

References:

Beauheim, R. L., G. J. Saulnier, Jr. and John D. Avis. 1990. **Interpretation of Brine-Permeability Tests of the Salado Formation at the Waste Isolation Pilot Plant Site: First Interim Report.** SAND90-0083. Albuquerque, NM: Sandia National Laboratories.

Beauheim, R. L., T. F. Dale, M. D. Fort, R. M. Roberts and W. A Stensrud. 1992. **Hydraulic Testing of Salado Formation Evaporites at the Waste Isolation Pilot Plant Site: Second Interpretive Report.** SAND92-0533. Albuquerque, NM: Sandia National Laboratories.

Gelbard, F. 1992. **A Two-Dimensional Model for Brine Flow to a Borehole in a Disturbed Rock Zone.** SAND92-1303. Albuquerque, NM: Sandia National Laboratories.

McTigue, D. F. 1992. **Permeability and Hydraulic Diffusivity of WIPP Repository Salt Inferred from Small-Scale Brine Inflow Experiments.** SAND92- . Albuquerque, NM: Sandia National Laboratories.

Table 1. Recommended Cumulative Probability Distributions
for formation permeability (m²), derived from
Figures 2-8.

Halite Far Field: Zone A

Permeability (m²)	Cumulative probability
0.0	0.00
1.0×10^{-24}	0.57
1.0×10^{-23}	0.71
1.0×10^{-22}	0.86
1.0×10^{-21}	1.00

Halite Depressurized Zone: Zones B and C

Permeability (m²)	Cumulative probability
1.0×10^{-22}	0.00
1.0×10^{-21}	0.44
1.0×10^{-20}	0.94
1.0×10^{-19}	1.00

Halite Disturbed Zone: Zones D and E

Permeability (m²)	Cumulative probability
1.0×10^{-18}	0.00
1.0×10^{-13}	1.00

Table 1. (Continued)

Anhydrite Far Field: Zone F

Permeability (m^2)	Cumulative probability
1.0×10^{-20}	0.00
1.0×10^{-19}	1.00

Anhydrite Depressurized Zone: Zones G and H

Permeability (m^2)	Cumulative probability
1.0×10^{-21}	0.00
1.0×10^{-20}	0.08
1.0×10^{-19}	0.58
1.0×10^{-18}	0.83
1.0×10^{-17}	0.92
1.0×10^{-16}	1.00

Anhydrite Disturbed Zone: Zone J

Permeability (m^2)	Cumulative probability
1.0×10^{-18}	0.00
1.0×10^{-17}	0.12
1.0×10^{-16}	0.25
1.0×10^{-15}	0.37
1.0×10^{-14}	0.75
1.0×10^{-13}	0.87
1.0×10^{-12}	1.00

Anhydrite Disturbed Zone: Zone I

Permeability (m^2)	Cumulative probability
1.0×10^{-19}	0.00
1.0×10^{-18}	1.00

Table 2.   Parameter Estimates from Borehole Experiments.   This from
information in Table 5 of an early draft of McTigue, 1992.   The
difference between the values from the early draft (this table) and
the table in McTigue, 1992 is the use of a literature value and a
WIPP-specific measured value, respectively, for brine
compressibility in the data interpretation.

Borehole #	Rock Type	Permeability @Po=10 MPa (m²)	Permeability @Po=5 MPa (m²)	Permeability @Po=01MPa (m²)	Diffusivity (m²/sec)
DBT10	Halite	2.9E-22±.18E-22	5.8E-22±.36E-22	2.9E-21±.18E-21	4.7E-11±.78E-11
DBT11	Halite	1.1E-21±.09E-21	2.3E-21±.18E-21	1.1E-20±.09E-20	3.5E-9±.63E-9
DBT12	Halite	6.4E-22±.72E-22	1.3E-21±.14E-21	6.4E-21±.72E-21	10E-8±.65E-8
DBT13	Halite	1.7E-22±.26E-22	3.4E-22±.32E-22	1.7E-21±.26E-21	5.9E-11±.2.3E-11
DBT14A	Halite	7.8E-22±.2.4E-22	1.6E-21±.48E-21	7.8E-21±.2.4E-21	2.8E-8±4.6E-8
DBT14B	Halite	2.2E-21±.28E-21	4.5E-21±.56E-21	2.2E-21±.28E-21	4.3E-8±3.3E-8
DBT15A	Halite	3.2E-22±.55E-22	6.4E-22±1.1E-22	3.2E-21±.55E-21	1.8E-10±.86E-10
DBT15B	Halite	1.8E-22±.59E-22	3.6E-22±1.1E-22	1.8E-21±.59E-21	1.3E-10±1.2E-10
L4B01	Halite	.67E-22±.43E-22	1.3E-22±.86E-22	.67E-21±.43E-21	5.8E-11±9.1E-11
DBT31A	Halite	9.0E-22±2.4E-22	1.8E-21±.48E-21	9.0E-21±.2.4E-21	1.27E-10±.22E-11
QPB01 *1	Anhydrite	4.8E-21±.3E-21	9.6E-21±.06E-21	4.8E-20±.3E-20	1.1E-8±.34E-8
QPB02 *1	Anhydrite	8.2E-20±.03E-20	1.6E-19±.006E-19	8.2E-19±.03E-19	1.2E-9±.014E-9
QPB03 *1	Anhydrite	4.8E-21±1.5E-21	9.6E-21±.3E-21	4.8E-20±1.5E-20	6.4E-7±18.8E-7*

*   The lower limit of these uncertainty bounds should be assumed to be zero.

*1 For all of these borehole tests, the length of the productive unit was assumed to be equal to the average

    thickness of Marker Bed 139 (3-feet).

2 of 2

Table 3: Compilation of Interpreted Values of Permeability, 1/5/92. Zones are referenced to Figure 1.

Zone Test   Measured Permeability   Pressure(MPA)

A. **HALITE FAR FIELD**

    QPP12 pre-mineby
                    6.8×10^{-22} m^2 9.5
    C2HO3   Too low to measure   not measureable
    SCP01 GZ   Too low to measure   not measureable
    QPP05   Too low to measure   not measureable
    QPP02   Too low to measure   not measureable

B. **HALITE DEPRESSURIZED ZONE**

    S1P72-A-GZ 8.6×10^{-22} m^2 5.1
    QPP21 post mineby
                    1.9×10^{-22} m^2 4.8
    C2H01-B 5.3×10^{-21} m^2 3.1
    C2H01-B-GZ 1.9×10^{-21} m^2 4.1
    L4P51-A 6.1×10^{-21} m^2 2.7
    S0P01 8.3×10^{-21} m^2 4.4
    S1P71-A 6.1×10^{-20} m^2 2.9
    QPP15 2.2×10^{-21} m^2 3.1
    DBT10 5.8×10^{-22} m^2 5.0 assumed
    DBT11 2.3×10^{-21} m^2 5.0 assumed
    DBT12 1.3×10^{-21} m^2 5.0 assumed
    DBT13 3.4×10^{-22} m^2 5.0 assumed
    DBT14A/B 3.1×10^{-21} m^2 5.0 assumed
    DBT15A/B 5.0×10^{-22} m^2 5.0 assumed
    L4B01 1.3×10^{-22} m^2 5.0 assumed
    DBT31A   not used
    QPP12 4.4×10^{-22} m^2 9.4

C. **HALITE DEPRESSURED ZONE**

Same as region B for permeability; linearly increase pressure from region E to Region A pressure.

D. **HALITE DISTURBED ROCK ZONE**

    C2H01-A 2.7×10^{-18} m^2 0.5
    C2H01-A-GZ   unmeasurable   0.0
    S1P73-B-GZ   unmeasureable   2.5

E. **HALITE DISTURBED ROCK ZONE**

Same as region D for permeability; linearly increase pressure from region I pressure to region C pressure.

Table 3: Compilation of Interpreted Values of Permeability, 1/5/92. Zones are referenced to Figure 1.

Zone	Test	Measured Permeability	Pressure(MPA)

A. HALITE FAR FIELD

	QPP12 pre-mineby		
		6.8×10^{-22} m^2	9.5
	C2HO3	Too low to measure	not measureable
	SCP01 GZ	Too low to measure	not measureable
	QPP05	Too low to measure	not measureable
	QPP02	Too low to measure	not measureable

B. HALITE DEPRESSURIZED ZONE

	S1P72-A-GZ	8.6×10^{-22} m^2	5.1
	QPP21 post mineby		
		1.9×10^{-22} m^2	4.8
	C2H01-B	5.3×10^{-21} m^2	3.1
	C2H01-B-GZ	1.9×10^{-21} m^2	4.1
	L4P51-A	6.1×10^{-21} m^2	2.7
	S0P01	8.3×10^{-21} m^2	4.4
	S1P71-A	6.1×10^{-20} m^2	2.9
	QPP15	2.2×10^{-21} m^2	3.1
	DBT10	5.8×10^{-22} m^2	5.0 assumed
	DBT11	2.3×10^{-21} m^2	5.0 assumed
	DBT12	1.3×10^{-21} m^2	5.0 assumed
	DBT13	3.4×10^{-22} m^2	5.0 assumed
	DBT14A/B	3.1×10^{-21} m^2	5.0 assumed
	DBT15A/B	5.0×10^{-22} m^2	5.0 assumed
	L4B01	1.3×10^{-22} m^2	5.0 assumed
	DBT31A	not used	
	QPP12	4.4×10^{-22} m^2	9.4

C. HALITE DEPRESSURED ZONE

Same as region B for permeability; linearly increase pressure from region E to Region A pressure.

D. HALITE DISTURBED ROCK ZONE

	C2H01-A	2.7×10^{-18} m^2	0.5
	C2H01-A-GZ	unmeasureable	0.0
	S1P73-B-GZ	unmeasureable	2.5

E. HALITE DISTURBED ROCK ZONE

Same as region D for permeability; linearly increase pressure from region I pressure to region C pressure.

Table 3. (Continued)

F. **ANHYDRITE FAR FIELD** (greater than 10 m from excavation)
    SCP01   MB 139
                        3.0×10^{-20} m^2 12.4
    QPP13 pre-mineby MB 139   12.5
                        4.1×10^{-20} m^2
    QPP03 pre mineby clay b
                        4.4×10^{-20} m^2 12.6

G. **ANHYDRITE DEPRESSURIZED ZONE** (less than 10 meters from excavation)
    C2H02 MB 139 7.8×10^{-20} m^2 9.3
    L4P51-B anhydrite c
                        5.0×10^{-20} m^2 5.1
    S1P71-B anhydrite c
                        6.8×10^{-20} m^2 4.9
    C2H01-C MB 139
                        9.5×10^{-19} m^2 8.0
    C1X10 MB 139 5.0×10^{-17} m^2 7.3
    QPP03 anhydrite b post mineby
                        7.9×10^{-20} m^2 7.0
    QPP13 MB 139 post mine-by
                        4.7×10^{-20} m^2 8.1
    L4P52-A anhydrite a
                        1.0×10^{-19} m^2 6.4
    QPB01 9.6×10^{-21} m^2 5.0 assumed
    QPB02 1.6×10^{-19} m^2 5.0 assumed
    QPB03 $1.2 \times 10^{--20}$ m^2 5.0 assumed
    S1P72   unmeasureable   1.2

H. **ANHYDRITE DEPRESSURIZED ZONE**
    Same permeability as region G; linearly increase pressure
    from region I or J pressure to region F pressure.

I. **ANHYDRITE DISTURBED ROCK ZONE (138)**
    S1P73-B MB 138 2.9×10^{-19} m^2 4.5

J. **ANHYDRITE DISTURBED ROCK ZONE**
    SOP01 GZ 5.7×10^{-18} m^2 0.5
    S1P73-A   too high to measure; estimated at 10^{-15} m^2
                                          0.0
    S1P73-A-GZ   too high to measure; estimated at 10^{-15} m^2
                                          0.0
    S1P71-A-GZ   too high to measure; estimated at 10^{-14} m^2
                                          0.0
    L4P51-A-GZ   too high to measure; estimated at 10^{-15} m^2
                                          0.3
    Crawley   1.6 to 3.2 $\times 10^{-13}$ m^2 ???

YET TO BE INTERPRETED

QPP01
QPP04
QPP11
QPP14
QPP22
QPP23
QPP24
QPP25
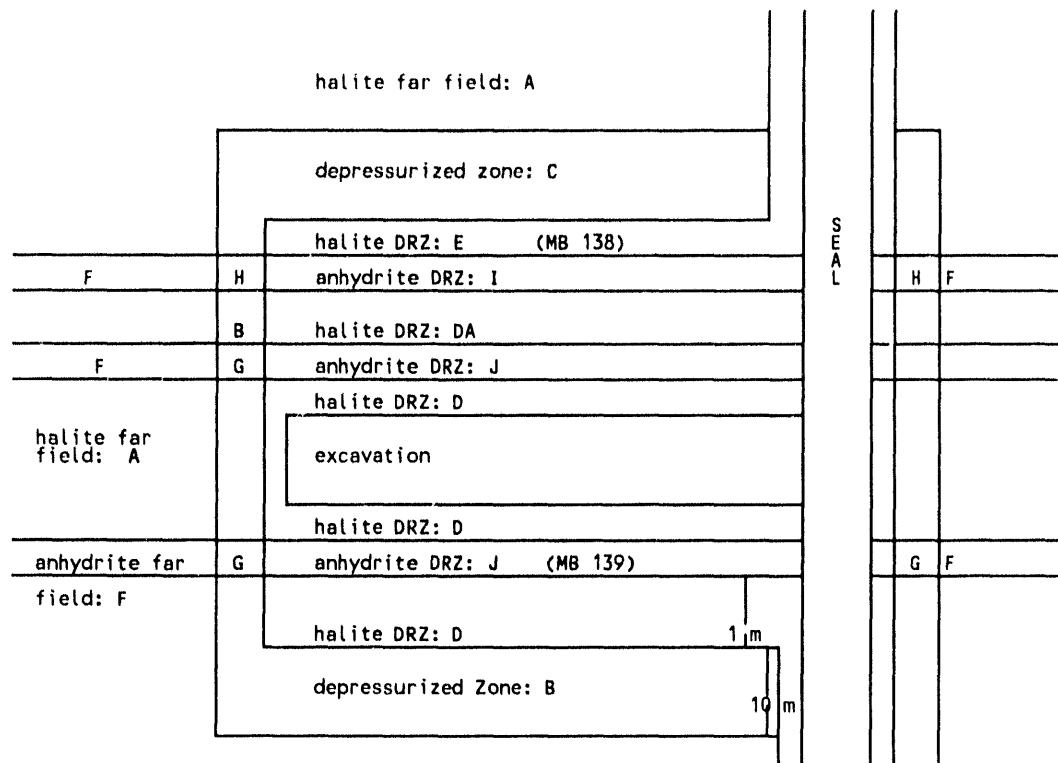
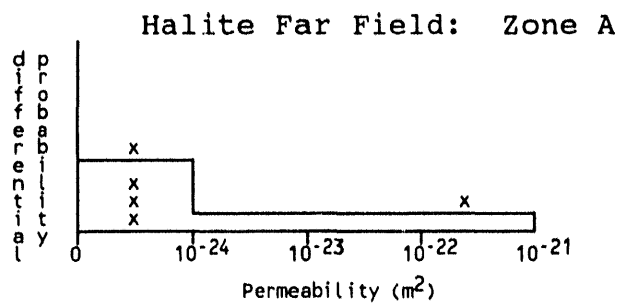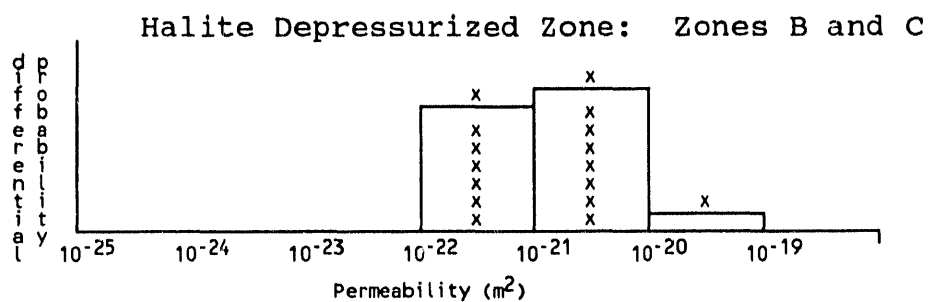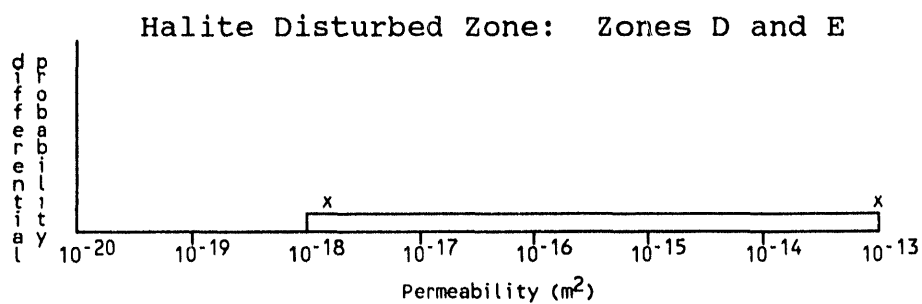Figure 1: Schematic for assigning flow properties to Salado Formation (Not to Scale!!!!)

Halite Far Field: Zone A

Figure 2.

Halite Depressurized Zone: Zones B and C

Figure 3.

Halite Disturbed Zone: Zones D and E

Figure 4.

Anhydrite Far Field: Zone F

Figure 5.

Anhydrite Depressurized Zone: Zones G and H

Figure 6.

Anhydrite Disturbed Zone: Zone J

Figure 7.

Anhydrite Disturbed Zone: Zone I
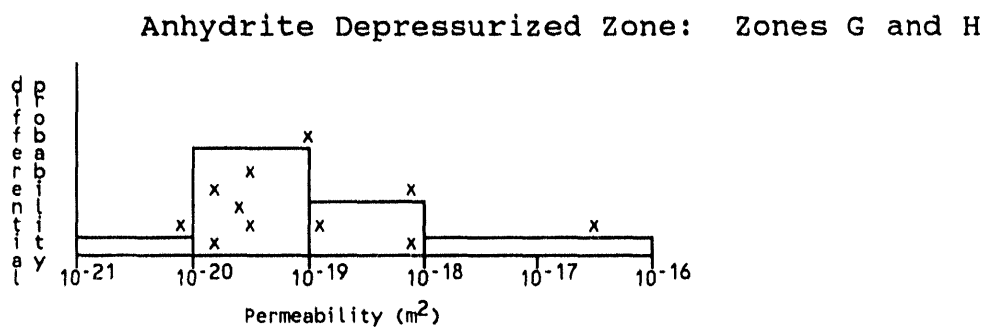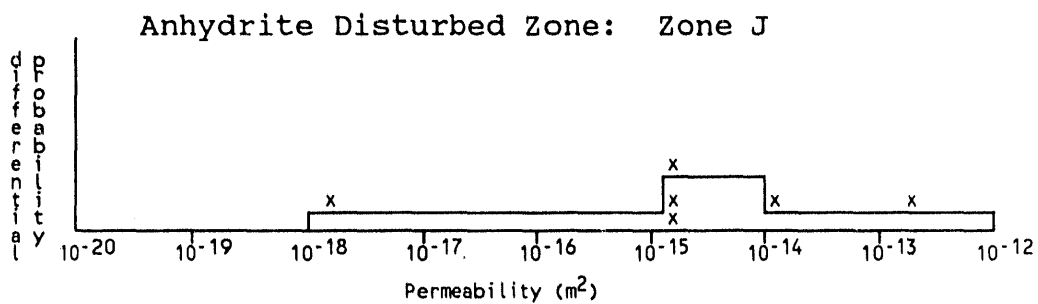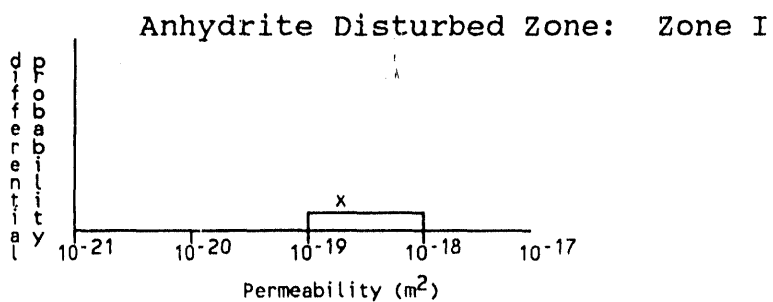

Figure 8.

A-19
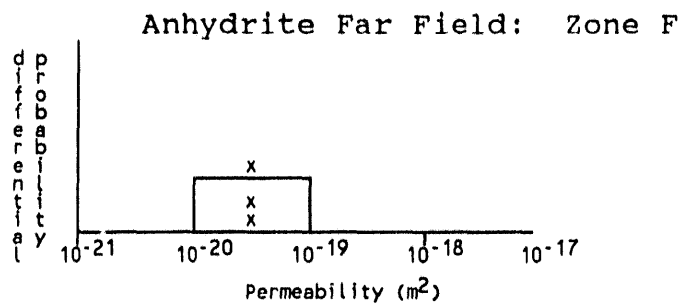
DISTRIBUTION

Federal Agencies

US Department of Energy (6)
Office of Civilian Radioactive Waste
  Management
Attn: Deputy Director, RW-2
        Associate Director, RW-10/50
         Office of Program and
        Resources Management
         Office of Contract Business
        Management
        Director, Analysis and
        Verification Division, RW-22
        Associate Director, RW-30
         Office of Systems and
        Compliance
        Associate Director, RW-40
         Office of Storage and
        Transportation
        Director, RW-4/5
         Office of Strategic Planning
        and International Programs
         Office of External Relations
Forrestal Building
Washington, DC 20585

US Department of Energy
Albuquerque Operations Office
Attn: National Atomic Museum Library
PO Box 5400
Albuquerque, NM 87185-5400

US Department of Energy (4)
WIPP Project Integration Office
Attn: W.J. Arthur III
        L.W. Gage
        P.J. Higgins
        D.A. Olona
PO Box 5400
Albuquerque, NM 87115-5400

US Department of Energy (3)
WIPP Project Integration Satellite
Office
Attn: R. Batra
        R. Becker
        B. Bliss
PO Box 3090, Mail Stop 525
Carlsbad, NM 88221-3090

US Department of Energy (3)
WIPP Project Site Office (Carlsbad)
Attn: V. Daub
        J. Lippis
        J.A. Mewhinney
PO Box 3090
Carlsbad, NM 88221-3090

US Department of Energy
Research & Waste Management Division
Attn: Director
PO Box E
Oak Ridge, TN 37831

US Department of Energy
Attn: E. Young
Room E-178
GAO/RCED/GTN
Washington, DC 20545

US Department of Energy
Office of Environmental Restoration
  and Waste Management
Attn: J. Lytle, EM-30,
         Trevion II
Washington, DC 20585-0002

US Department of Energy (3)
Office of Environmental Restoration
  and Waste Management
Attn: M. Frei, EM-34,
         Trevion II
Washington, DC 20585-0002

US Department of Energy
Office of Environmental Restoration
  and Waste Management
Attn: S. Schneider, EM-342,
         Trevion II
Washington, DC 20585-0002

US Department of Energy (2)
Office of Environment, Safety
  and Health
Attn: C. Borgstrom, EH-25
        R. Pelletier, EH-231
Washington, DC 20585

US Department of Energy (2)
Idaho Operations Office
Fuel Processing and Waste
  Management Division
785 DOE Place
Idaho Falls, ID 83402

US Environmental Protection
  Agency (2)
Radiation Protection Programs
Attn: M. Oge
ANR-460
Washington, DC 20460

US Geological Survey (2)
Water Resources Division
Attn: R. Livingston
4501 Indian School NE
Suite 200
Albuquerque, NM 87110

US Nuclear Regulatory Commission
Division of Waste Management
Attn: H. Marson
Mail Stop 4-H-3
Washington, DC 20555

Boards

Defense Nuclear Facilities Safety
Board
Attn: D. Winters
625 Indiana Ave. NW, Suite 700
Washington, DC 20004

Nuclear Waste Technical Review
Board (2)
Attn: Chairman
        S.J.S. Parry
1100 Wilson Blvd., Suite 910
Arlington, VA 22209-2297

Advisory Committee on Nuclear
Waste
Nuclear Regulatory Commission
Attn: R. Major
7920 Norfolk Ave.
Bethesda, MD 20814

State Agencies

Environmental Evaluation Group (3)
Attn: Library
7007 Wyoming NE
Suite F-2
Albuquerque, NM 87109

NM Bureau of Mines and Mineral
   Resources
Socorro, NM 87801

NM Energy, Minerals, and Natural
   Resources Department
Attn: Library
2040 S. Pacheco
Santa Fe, NM 87505

NM Environment Department (3)
Secretary of the Environment
Attn: J. Espinosa
1190 St. Francis Drive
Santa Fe, NM 87503-0968

NM Environment Department
WIPP Project Site
Attn: P. McCasland
PO Box 3090
Carlsbad, NM 88221

Laboratories/Corporations

Battelle Pacific Northwest
Laboratories
Attn: R.E. Westerman, MSIN P8-44
Battelle Blvd.
Richland, WA 99352

INTERA Inc.
Attn: J.F. Pickens
6850 Austin Center Blvd.
Suite 300
Austin, TX 78731

INTERA Inc.
Attn: W. Stensrud
PO Box 2123
Carlsbad, NM 88221

IT Corporation
Attn: R.F. McKinney
Regional Office
5301 Central NE, Suite 700
Albuquerque, NM 87108

Los Alamos National Laboratory
Attn: B. Erdal, CNC-11
PO Box 1663
Los Alamos, NM 87544

RE/SPEC, Inc.
Attn: W. Coons
4775 Indian School NE
Suite 300
Albuquerque, NM 87110-3927

RE/SPEC, Inc. (2)
Attn: N.S. Brodsky
        J.L. Ratigan
PO Box 725
Rapid City, SD 57709

Rock Physics Associates
Attn: J.D. Wells
4320 Stevens Creek Blvd. Ste. 282
San Jose, CA 95129

Southwest Research Institute (2)
Center for Nuclear Waste
   Regulatory Analysis
Attn: P.K. Nair
6220 Culebra Road
San Antonio, TX 78228-0510

SAIC
Attn: D.C. Royer
101 Convention Center Dr.
Las Vegas, NV 89109

SAIC
Attn: H.R. Pratt
10260 Campus Point Dr.
San Diego, CA 92121

SAIC (2)
Attn: M. Davis
       J. Tollison
2109 Air Park Rd. SE
Albuquerque, NM 87106

Tech Reps Inc. (4)
Attn: J. Chapman
       C. Crawford
       V. Gilliland
       T. Peterson
5000 Marble NE, Suite 222
Albuquerque, NM 87110

TRW Environmental Safety Systems
Attn: L. Wildman
2650 Park Tower Dr., Suite 1300
Vienna, VA 22180-7306

Westinghouse Electric Corporation (5)
Attn: Library
       C. Cox
       L. Fitch
       B.A. Howard
       R. Kehrman
PO Box 2078
Carlsbad, NM 88221

Westinghouse-Savannah River
Technology Center (4)
Attn: N. Bibler
       J.R. Harbour
       M.J. Plodinec
       G.G. Wicks
Aiken, SC 29802

National Academy of Sciences, WIPP Panel

Howard Adler
Oak Ridge Associated Universities
Medical Sciences Division
PO Box 117
Oak Ridge, TN 37831-0117

Ina Alterman
Board on Radioactive
  Waste Management, GF456
2101 Constitution Ave.
Washington, DC 20418

Fred M. Ernsberger
250 Old Mill Road
Pittsburgh, PA 15238

John D. Bredehoeft
Western Region Hydrologist
Water Resources Division
US Geological Survey (M/S 439)
345 Middlefield Road
Menlo Park, CA 94025

Rodney C. Ewing
Department of Geology
University of New Mexico
Albuquerque, NM 87131

Charles Fairhurst, Chairman
Department of Civil and
  Mineral Engineering
University of Minnesota
500 Pillsbury Dr. SE
Minneapolis, MN 55455-0220

B. John Garrick
PLG Incorporated
4590 MacArthur Blvd., Suite 400
Newport Beach, CA 92660-2027

Leonard F. Konikow
US Geological Survey
431 National Center
Reston, VA 22092

Peter B. Myers
National Academy of Sciences
Board on Radioactive
  Waste Management
2101 Constitution Ave.
Washington, DC 20418

Jeremiah O'Driscoll
Jody Incorporated
505 Valley Hill Drive
Atlanta, GA 30350

Christopher G. Whipple
Clement International
160 Spear St., Suite 1380
San Francisco, CA 94105

Individuals

P. Drez
8816 Cherry Hills Rd. NE
Albuquerque, NM 87111

D.W. Powers
Star Route Box 87
Anthony, TX 79821

Universities

University of New Mexico
Geology Department
Attn: Library
Albuquerque, NM 87131

University of Washington
College of Ocean
  and Fishery Sciences
Attn: G.R.Heath
583 Henderson Hall
Seattle, WA 98195

Libraries

Thomas Brannigan Library
Attn: D. Dresp
106 W. Hadley St.
Las Cruces, NM 88001

Government Publications Department
Zimmerman Library
University of New Mexico
Albuquerque, NM 87131

Hobbs Public Library
Attn: M. Lewis
509 N. Ship St.
Hobbs, NM 88248

New Mexico Junior College
Pannell Library
Attn: R. Hill
Lovington Highway
Hobbs, NM 88240

New Mexico State Library
Attn: N. McCallan
325 Don Gaspar
Santa Fe, NM 87503

New Mexico Tech
Martin Speere Memorial Library
Campus Street
Socorro, NM 87810

WIPP Public Reading Room
Carlsbad Public Library
Attn: Director
101 S. Halagueno St.
Carlsbad, NM 88220

Foreign Addresses

Studiecentrum Voor Kernenergie
Centre D'Energie Nucleaire
Attn: A. Bonne
SCK/CEN   Boeretang 200
B-2400 Mol, BELGIUM

Atomic Energy of Canada, Ltd. (3)
Whiteshell Research Estab.
Attn: B. Goodwin
      M. Stevens
      D. Wushke
Pinewa, Manitoba, CANADA ROE 1L0

Francois Chenevier (2)
ANDRA
Route du Panorama Robert Schumann
B.P. 38
92266 Fontenay-aux-Roses, Cedex
FRANCE

Jean-Pierre Olivier
OECD Nuclear Energy Agency
Division of Radiation Protection
  and Waste Management
38, Boulevard Suchet
75016 Paris, FRANCE

Claude Sombret
Centre D'Etudes Nucleaires
  De La Vallee Rhone
CEN/VALRHO
S.D.H.A.   B.P. 171
30205 Bagnols-Sur-Ceze, FRANCE

Gesellschaft fur Reaktorsicherheit
(GRS) (2)
Attn: B. Baltes
      W. Muller
Schwertnergasse 1
D-5000 Cologne, GERMANY

Bundesanstalt fur Geowissenschaften
  und Rohstoffe
Attn: M. Langer
Postfach 510 153
3000 Hanover 51, GERMANY

Bundesministerium fur Forschung und
   Technologie
Postfach 200 706
5300 Bonn 2, GERMANY

Institut fur Tieflagerung (2)
Attn: K. Kuhn
Theodor-Heuss-Strasse 4
D-3300 Braunschweig, GERMANY

Physikalisch-Technische Bundesanstalt
Attn: P. Brenneke
Postfach 3345
D-3300 Braunschweig, GERMANY

Shingo Tashiro
Japan Atomic Energy Research Inst.
Tokai-Mura, Ibaraki-Ken, 319-11
JAPAN

Netherlands Energy Research
Foundation ECN
Attn: L.H. Vons
3 Westerduinweg
PO Box 1
1755 ZG Petten, THE NETHERLANDS

Svensk Karnbransleforsorjning AB
Attn: F. Karlsson
Project KBS
Karnbranslesakerhet
Box 5864
10248 Stockholm, SWEDEN

Nationale Genossenschaft für die
Lagerung radioaktiver Abfälle (2)
Attn: S. Vomvoris
      P. Zuidema
Hardstrasse 73
CH-5430 Wettingen, SWITZERLAND

AEA Technology
Attn: J.H. Rees
D5W/29 Culham Laboratory
Abington, Oxfordshire OX14 3DB
UNITED KINGDOM

AEA Technology
Attn: W.R. Rodwell
044/A31 Winfrith Technical Centre
Dorchester, Dorset DT2 8DH
UNITED KINGDOM

AEA Technology
Attn: J.E. Tinson
B4244 Harwell Laboratory
Didcot, Oxfordshire OX11 ORA
UNITED KINGDOM

D.R. Knowles
British Nuclear Fuels, plc
Risley, Warrington, Cheshire WA3 6AS
1002607 UNITED KINGDOM

Internal

1502	J.C. Cummings
6000	D.L. Hartley
6115	R.L. Beauheim
6115	P.B. Davies
6116	D.J. Borns
6117	D.J. Holcomb
6117	D.H. Zeuch
6119	E.D. Gorham
6119	S.M. Howarth (15)
6119	Staff (14)
6121	J.R. Tillerson
6121	Staff (7)
6300	D.E. Ellis
6302	L.E. Shephard
6303	S.Y. Pickering
6303	W.D. Weart
6305	S.A. Goldstein
6305	A.R. Lappin
6306	A.L. Stevens
6342	D.R. Anderson
6342	Staff (20)
6343	V. Harper-Slaboszewicz
6343	Staff (2)
6345	R.C. Lincoln
6345	Staff (9)
6347	D.R. Schafer
6348	J.T. Holmes
6348	Staff (4)
6351	R.E. Thompson
6352	D.P. Garber
6352	S.E. Sharpton
6352	WIPP Central Files (10)
7141	Technical Library (5)
7151	Technical Publications
7613-2	Document Processing for DOE/OSTI (10)
8523-2	Central Technical Files

DATE
FILMED
11 / 22 / 93
END